

Modeling the influence of nutrients, turbulence and grazing on *Pfiesteria* population dynamics

Raleigh R. Hood^{a,*}, Xinsheng Zhang^{a,b}, Patricia M. Glibert^a,
Michael R. Roman^a, Diane K. Stoecker^a

^a Horn Point Laboratory, University of Maryland Center for Environmental Science, P.O. Box 775,
2020 Horns Point Road, Cambridge, MD 21613, USA

^b NOAA Chesapeake Bay Office, Cooperative Oxford Laboratory, 904 South Morris Street, Oxford, MD 21654, USA

Received 22 January 2006; received in revised form 23 April 2006; accepted 28 April 2006

Abstract

A semi-idealized marine ecosystem model, designed as a heuristic tool for exploring the population dynamics of non-inducible versus toxic forms of *Pfiesteria* is described. The model is based on empirical evidence suggesting that these differing functional types of *Pfiesteria* also differ substantially in terms of what they eat and how they utilize it to optimize their growth. Non-inducible strains are similar to other mixotrophic dinoflagellates, whereas toxic strains may consume organic matter and detritus, produce toxins and attack fish. In our model formulation we represent these differences in a simplified way: the non-inducible strain is kleptochloroplastidic and it can take up DIN, but it cannot utilize DON, whereas the toxic strain is heterotrophic, it cannot utilize DIN, but it can utilize DON directly. These differences give rise to very different impacts on prey and nutrient concentrations in our model. Under high DIN/DON ratio conditions, the non-inducible cells grew much faster and were therefore more likely to bloom, but this advantage is substantially mitigated when the DIN/DON ratio is low. A turbulence parameterization was also incorporated into our model. The effect of this was to reduce the grazing rate of *Pfiesteria* when turbulence levels are high. According to our model, increased turbulence is more detrimental to the toxic functional type because it grows more slowly. The further imposition of microzooplankton grazing in the model showed that top-down control effects can be very significant, which is consistent with both laboratory and field studies and the general idea that plankton blooms can only happen in the absence of substantial grazing control. In general, our model results suggest that non-toxic blooms are more likely to occur in more turbulent inorganic-nutrient rich conditions, which are often found in more open coastal and estuarine waters that are subject to high inorganic loading. In contrast, toxic blooms are more likely to occur in calm, organic-nutrient rich conditions, which are often found in shallow, protected tributaries that are subject to high organic nutrient loading. Our model results also support the idea that the absence of strong grazing pressure is a prerequisite to bloom formation for both non-inducible and toxic strains of *Pfiesteria*. These results are generally consistent with observed patterns of toxic *Pfiesteria* blooms in Chesapeake Bay, the Neuse River of North Carolina and many other coastal and estuarine environments.

© 2006 Elsevier B.V. All rights reserved.

Keywords: *Pfiesteria*; Ecosystem model; Zooplankton grazing; Turbulence; Nutrients; DIN; DON

1. Introduction

Harmful algae blooms (HABs) have been increasing in frequency worldwide (Anderson, 1989; Smayda, 1990; Hallegraeff, 1993; Glibert et al., 2005a). Coastal

* Corresponding author. Tel.: +1 410 221 8434;
fax: +1 410 221 8490.

E-mail address: rhoo@hpl.umces.edu (R.R. Hood).

eutrophication is one of the causes of this proliferation (Smayda, 1990; Glibert et al., 2005b), but a variety of factors are known to influence HABs. These include inorganic and organic nutrient concentration and/or ratios, as well as light, temperature and salinity, stratification and grazing pressure (Glibert et al., 2005a). Moreover, many HAB species have benthic stages (e.g., cysts) that influence where and when blooms occur (e.g. Anderson, 1989; Burkholder et al., 2001a). For most HAB species the specific combination of factors that lead to harmful blooms is unknown. It is not surprising, then, that efforts to develop mechanistic models for predicting HABs have not been particularly successful. Mechanistic ecosystem models that can reliably predict monospecific HAB outbreaks are few. However, mechanistic models can play an important heuristic role in helping us understand how different environmental factors might influence bloom formation in situ (e.g., Anderson et al., 2002; Zhang et al., 2004).

Pfiesteria piscicida is a mixotrophic HAB species that has a complex life cycle including flagellated, amoeboid, and encysted stages (Burkholder and Glasgow, 1997; Burkholder et al., 2001a). In addition to this complex life cycle, the feeding behavior and toxicity of *Pfiesteria* appears to vary substantially in response to environmental conditions, i.e., ranging from more benign mixotrophic forms that produce little or no toxin (the so-called “non-inducible” strains, Burkholder et al., 2001b), to much more aggressive toxic forms that exhibit striking swarming behavior and can even attack fish (Burkholder et al., 2001a; Vogelbein et al., 2002; Gordon and Dyer, 2005). *Pfiesteria* has been implicated as one of the causative agents of numerous fish kills in the coastal waters of the southeastern U.S. (Lewitus et al., 1995; Burkholder and Glasgow, 1997; Magnien, 2001). However, as a result of all of these life cycle and nutritional complexities (and the fact that the more toxic forms can only be cultured and manipulated using specialized biohazard culturing facilities), studying *P. piscicida* physiology and population dynamics has posed a significant scientific challenge. It is premature to attempt the development of a prognostic model for this species. However, as we show in this paper, a mechanistic model can be gainfully applied as a heuristic tool.

Substantial progress has been made in recent years toward developing a deeper understanding of the physiological ecology of *Pfiesteria*. These studies have helped to clarify the influences of organic and inorganic nutrient concentrations and ratios (Lewitus et al., 1999a,b; Glibert et al., 2006; Skelton et al., 2006),

food abundance and quality (Stoecker et al., 2002; Lewitus et al., 2006), grazing control (Roman et al., 2006) and the role of turbulence (Stoecker et al., 2006). Taken together, these studies suggest that *Pfiesteria* blooms are more likely to occur under stratified conditions when organic nutrient concentrations are high, and top-down grazing losses are minimized. Nonetheless, the specific combination of factors that give rise to *Pfiesteria* blooms in situ is still unclear. As with all HAB species (and most ecological phenomena), multiple factors are usually involved in bloom formation, whereas experimental studies often only allow manipulation of one variable at a time (Glibert and Burkholder, 2006). Mechanistic ecosystem models provide a powerful means of synthesizing and integrating results from a suite of experimental studies into a single framework that can then be used to study the interaction of multiple environmental and physiological factors on *Pfiesteria* population dynamics.

In this paper we describe a heuristic nitrogen-based ecosystem model that utilizes field observations, laboratory/experimental results and literature data, which was developed to study *Pfiesteria* population dynamics. The model is composed of *Pfiesteria* zoospores, microzooplankton, mesozooplankton (modeled based on *Acartia* dynamics), dissolved inorganic nitrogen (DIN), dissolved organic nitrogen (DON), diatom, cryptophytes, and detritus (Fig. 1). In addition to modeling the total biomass of *Pfiesteria*, our model simulates the time dependency of both individual body size and abundance of *Pfiesteria* zoospores, and can represent both non-inducible (NON-IND) and toxic (TOX-A, sensu Burkholder et al., 2001a,b) *Pfiesteria* functional types by specifying differences in grazing rate, kleptoplastidy, DON utilization and top-down control. In the pages that follow we describe the basis of

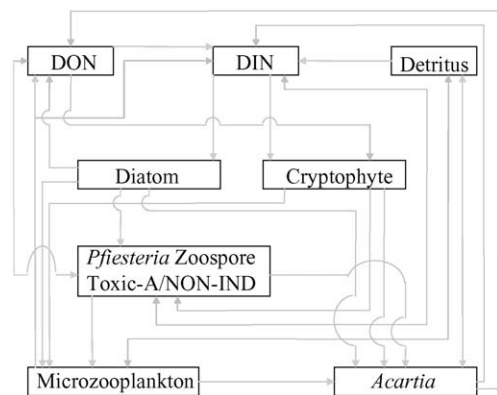


Fig. 1. A schematic diagram of the generalized eight-compartment *Pfiesteria* model.

the model formulation and parameterization, and we carry out a series of modeling “experiments” that are designed to answer a suite of specific questions about the potential effects of several different physical, chemical, and biological factors and processes on *Pfiesteria* population dynamics.

2. The model

This model, which has eight state variables (Fig. 1, Table 1), is based on the assumption that dinoflagellate population dynamics are a function of nutrients (particulate/dissolved, inorganic/organic), predation (microzooplankton and mesozooplankton) and turbulence. The mass in each compartment is expressed in μM nitrogen. In addition, *Pfiesteria* zoospores’ cell size (M_{size}) and abundance (M_{num}) are expressed in pmol nitrogen cell^{-1} and cells mL^{-1} , respectively. Note that the cell size and abundance equations, and many other aspects of this model, are based upon a simpler version described by Zhang et al. (2003). Both here and in Zhang et al. (2003) the formulation and parameterization of the model components involving *Pfiesteria* are based on the current understanding of the physiology and ecology of this organism, but also, by necessity, are highly simplified and depend on the somewhat limited data availability. In many cases, functional relationships and parameterizations had to be adopted from other organisms or assumed (see Table 1 and legend explanations). The formulation and parameterization of NON-IND and TOX-A functional types are based upon a simple conceptual model, i.e., NON-IND zoospores are considered to be kleptochloroplastidic and to therefore have more autotrophic characteristics than TOX-A zoospores, which have more heterotrophic characteristics. The specific differences between the modeled NON-IND and TOX-A functional types are specified in Table 2.

2.1. Zoospores

The rate of change of zoospore biomass (M) reflects the balance between herbivorous grazing and nutrient uptake, and losses through expulsion (i.e., rejection of particulate food waste by a single-celled organism from food vacuoles as opposed to egestion), excretion, microzooplankton grazing, mesozooplankton (as *Acartia*) grazing, and natural mortality

$$\begin{aligned} dM/dt = & \text{GRAZING}_m + \text{UPTAKE}_m - \text{EXPULSION}_m \\ & - \text{EXCRETION}_m - \text{GRAZING}_m \\ & - \text{GRAZING}_{mz_2} - \text{MORTALITY}_m \end{aligned} \quad (1)$$

Based on the origin of the food sources, the grazing rate for zoospores (GRAZING_m) can be separated into grazing rate on diatoms, cryptophytes, and DON (the latter for TOX-A only). Cryptophytes are known to be a preferred algal food for *Pfiesteria* (e.g. Lewitus et al., 1999b). The diatom term is meant to represent all non-cryptophyte grazing (Table 1). In this model, we can also set a grazing threshold for each food source (i) below which grazing stops. However, in the simulations presented in this paper the grazing thresholds are all set to zero (Table 1). A saturating hyperbolic expression is used to define the grazing rate for zoospores

$$\text{GRAZING}_m = \sum \text{GRAZING}_{im} \quad (2)$$

$$\text{If } i \leq \text{TH}_{im}$$

$$\text{GRAZING}_{im} = 0 \quad (3A)$$

else

$$\begin{aligned} \text{GRAZING}_{im} \\ = \exp(-0.2038 \times S_{\text{rate}}) \times G_{\text{mm}} \times i \times O_{im} \\ \times M/\text{THETA}_m \end{aligned} \quad (3B)$$

$$\text{THETA}_m = O_{\text{pm}} \times P + O_{\text{p}_2m} \times P_2 + O_{\text{n}_2m} \times N_2 + \text{MK}_s \quad (4)$$

For simplicity, we assume that the value of the coefficient O_{n_2m} is equal to 1 and 0 for TOX-A and NON-IND, respectively, i.e., TOX-A consumes DON and NON-IND does not. Data of Burkholder et al. (2001a) and Glibert et al. (2006) generally support this assumption. For example, Burkholder found that NON-IND cultures increased an order of magnitude when exposed to inorganic nutrients, but TOX-A did not, and Glibert et al. (2006) observed DON to be a preferred N source for TOX-A cultures, even though overall uptake rates were low. In this model, TOX-A can grow on DON even without PON food. Note that we can assign the value of O_{n_2m} to be less than 1 and larger than 0 to represent any *Pfiesteria* zoospore strains that might lie somewhere in between our idealized TOX-A and NON-IND strains in terms of grazing rates.

GRAZING_{im} , TH_{im} , and O_{im} are the grazing rate, the grazing threshold, and the grazing preference (which scale from 0 to 1) for zoospores feeding on diatom ($i = p$), cryptophyte ($i = p_2$), and DON ($i = n_2$), respectively. G_{mm} is the maximum specific rate for zoospore grazing, MK_s is the half-saturation constant for zoospore grazing, and S_{rate} is a shear rate that modifies the grazing rate of the zoospores as a function of turbulence. Shear due to turbulence is one of the factors

Table 1
Model parameters, initial conditions and sources

Description	Symbol	Value	Units	Source
Irradiance	I	83	$\mu\text{E m}^{-2} \text{s}^{-1}$	1
Light hour	LightHour	12	h	1
Dark hour	DarkHour	12	h	1
Shear rate (low)	S_{rate}	0	s^{-1}	2
Shear rate (high)	S_{rate}	3	s^{-1}	2
Zoospores (M)				
Zoospore biomass	M	0.35	$\mu\text{M N}$	1
Zoospore abundance	M_{num}	500	cell ml^{-1}	1
Zoospore size	M_{size}	0.7	pmol N cell^{-1}	1
Maximal zoospore size	M_{max}	1.4	pmol N	1
Critical zoospore size	M_{cri}	0.5	pmol N	1
Zoospore specific mortality rate (normal)	S_{m}	0.18	Day^{-1}	3
Zoospore specific mortality rate (starvation)	S_{m}	0.5	Day^{-1}	1
Maximum zoospore specific grazing rate (NON-IND)	G_{mm}	5.00	Day^{-1}	1
Maximum zoospore specific grazing rate (TOX-A)	G_{mm}	1.70	Day^{-1}	4
Half-saturation constant for zoospore grazing	MK_{s}	3.00	$\mu\text{M N}$	1
Assimilation efficiency of M on diatom	AE_{pm}	0.70	–	5
Assimilation efficiency of M on cryptophyte	AE_{p2m}	0.70	–	5
Assimilation efficiency of M on DON	AE_{n2m}	1	–	6
Active excretion efficiency of M on diatom	AEX_{pm}	0.30	–	7
Active excretion efficiency of M on cryptophyte	AEX_{p2m}	0.30	–	7
Active excretion efficiency of M on DON	AEX_{n2m}	0.30	–	7
Zoospore basal specific excretion rate	BEX_{m}	0.1	Day^{-1}	1
Zoospore feeding preference on diatom	O_{pm}	0.3	–	8
Zoospore feeding preference on cryptophyte	O_{p2m}	1	–	8
Zoospore feeding preference on DON for TOX-A	O_{n2m}	1	–	8
Zoospore feeding preference on DON for NON-IND	O_{n2m}	0	–	9
Zoospore feeding threshold on diatom	TH_{pm}	0 (off)	$\mu\text{M N}$	10
Zoospore feeding threshold on cryptophyte	TH_{p2m}	0 (off)	$\mu\text{M N}$	10
Zoospore feeding threshold on DON	TH_{n2m}	0 (off)	$\mu\text{M N}$	10
Light saturation parameter for zoospore	$I_{K_{\text{m}}}$	75	$\mu\text{E m}^{-2} \text{s}^{-1}$	11
Maximum zoosp. specific DIN uptake rate (NON-IND)	μ_{mm}	1.42	Day^{-1}	12
Maximum zoosp. specific DIN uptake rate (TOX-A)	μ_{mm}	0	Day^{-1}	13
Half-saturation constant for zoosp. DIN uptake	MPK_{s}	2.0	$\mu\text{M N}$	12
Diatom (P)				
Diatom biomass	P	1.4	$\mu\text{M N}$	1
Diatom specific mortality rate	S_{p}	0.12	Day^{-1}	1
Maximum diatom specific DIN uptake rate	μ_{mp}	2.5	Day^{-1}	14
Half-saturation const. for diatom DIN uptake	PK_{s}	1.0	$\mu\text{M N}$	14
Light saturation parameter for diatom	$I_{K_{\text{p}}}$	50	$\mu\text{E m}^{-2} \text{s}^{-1}$	15
Maximum diatom specific DIN uptake rate (dark)	μ_{mpd}	0 (off)	Day^{-1}	16
Half-saturation constant for diatom DIN uptake (dark)	PK_{sd}	0.50	$\mu\text{M N}$	17
DON exudation fraction for diatoms	α	0.2	–	18
Cryptophyte (P_2)				
Cryptophyte biomass	P_2	1.40	μM	19
Cryptophyte specific mortality rate	S_{p2}	0.12	Day^{-1}	20
Maximum cryptophyte DIN uptake rate	μ_{mnp2}	1.42	Day^{-1}	21
Half-saturation const. for cryptophyte DIN uptake	P_2K_{sn}	1.0	$\mu\text{M N}$	21
Maximum cryptophyte DIN uptake rate (dark)	μ_{mnp2d}	0 (off)	Day^{-1}	16
Half-saturation const. for cryptophyte DIN uptake (dark)	P_2K_{snd}	0.50	$\mu\text{M N}$	17
Light saturation param. for cryptophyte DIN uptake	$I_{K_{\text{np2}}}$	30	$\mu\text{E m}^{-2} \text{s}^{-1}$	22
Maximum cryptophyte DON uptake rate	μ_{mn2p2}	1.42	Day^{-1}	23
Half-saturation const. for cryptophyte DON uptake	P_2K_{sn2}	1.0	$\mu\text{M N}$	23
Maximum cryptophyte DON uptake rate (dark)	μ_{mn2p2d}	0 (off)	Day^{-1}	16
Half-saturation const. for cryptophyte DON uptake (dark)	P_2K_{sn}	0.50	$\mu\text{M N}$	17

Table 1 (Continued)

Description	Symbol	Value	Units	Source
Light saturation param. for cryptophyte DON uptake	$I_{K_{n_2p_2}}$	30	$\mu\text{E m}^{-2} \text{s}^{-1}$	23
Dissolved inorganic Nitrogen (N)				
DIN concentration	N	20	$\mu\text{M N}$	24
Partitioning parameter zoospore excretion	GAMMA_m	0.8	–	25
Partitioning parameter for microzooplankton excretion	GAMMA_z	0.8	–	25
Partitioning parameters for <i>Acartia</i> excretion	GAMMA_{z_2}	0.8	–	25
Detritus specific remineralization rate	e	0.05	Day^{-1}	1
Dissolved organic Nitrogen (N_2)				
DON concentration	N_2	1	$\mu\text{M N}$	24
DON specific remineralization rate	e_2	0.05	Day^{-1}	26
Microzooplankton (Z)				
Microzooplankton biomass	Z	1	$\mu\text{M N}$	19
Microzooplankton specific mortality rate	S_z	0.05	Day^{-1}	27
Assimilation efficiency for Z on diatom	AE_{pz}	0.70	–	27
Assimilation efficiency for Z on cryptophyte	AE_{p_2z}	0.70	–	27
Assimilation efficiency for Z on zoospore	AE_{mz}	0.70	–	27
Assimilation efficiency for Z on detritus	AE_{dz}	0.35	–	27
Growth efficiency for Z on diatom	GE_{pz}	0.30	–	27
Growth efficiency for Z on cryptophyte	G_{ep_2z}	0.30	–	27
Growth efficiency for Z on zoospore	GE_{mz}	0.30	–	27
Growth efficiency for Z on detritus	GE_{dz}	0.15	–	27
Maximum microzooplankton grazing rate	G_{mz}	6.0	Day^{-1}	28
Half-saturation const. for microzooplankton grazing	ZK_s	6.0	$\mu\text{M N}$	28
Microzooplankton feeding preference on diatom	O_{pz}	0.3	–	29
Microzooplankton feeding preference on cryptophyte	O_{p_2z}	1	–	29
Microzooplankton feeding preference on zoospore for NON-IND	O_{mz}	1	–	29
Microzooplankton feeding preference on zoospore for TOX-A	O_{mz}	0.2	–	29
Microzooplankton feeding preference on detritus	O_{dz}	1	–	29
Microzooplankton grazing threshold on diatom	TH_{pz}	0 (off)	$\mu\text{M N}$	9
Microzooplankton grazing threshold on cryptophyte	TH_{p_2z}	0 (off)	$\mu\text{M N}$	9
Microzooplankton grazing threshold on zoospore	TH_{mz}	0 (off)	$\mu\text{M N}$	9
Microzooplankton grazing threshold on detritus	TH_{dz}	0 (off)	$\mu\text{M N}$	9
<i>Acartia</i> (Z_2)				
<i>Acartia</i> biomass	Z_2	1	$\mu\text{M N}$	30
<i>Acartia</i> specific mortality rate	S_{z_2}	0.05	Day^{-1}	27
Assimilation efficiency for Z_2 on diatom	AE_{pz_2}	0.70	–	27
Assimilation efficiency for Z_2 on cryptophyte	$\text{AE}_{p_2z_2}$	0.70	–	27
Assimilation efficiency for Z_2 on zoospore	AE_{mz_2}	0.70	–	27
Assimilation efficiency for Z_2 on microzooplankton	AE_{zz_2}	0.70	–	27
Assimilation efficiency for Z_2 on detritus	AE_{dz_2}	0.35	–	27
Growth efficiency for Z_2 on diatom	GE_{pz_2}	0.30	–	27
Growth efficiency for Z_2 on cryptophyte	$\text{G}_{ep_2z_2}$	0.30	–	27
Growth efficiency for Z_2 on zoospore	GE_{mz_2}	0.30	–	27
Growth efficiency for Z_2 on microzooplankton	G_{Ezz_2}	0.30	–	27
Growth efficiency for Z_2 on detritus	G_{Edz_2}	0.15	–	27
Maximum <i>Acartia</i> specific grazing rate	G_{mz_2}	4.00	Day^{-1}	31
Half-saturation constant for <i>Acartia</i> grazing	Z_2K_s	12.0	$\mu\text{M N}$	32
<i>Acartia</i> feeding preference on diatom	O_{pz_2}	1	–	32
<i>Acartia</i> feeding preference on cryptophyte	$O_{p_2z_2}$	1	–	32
<i>Acartia</i> feeding preference on zoospore for NON-IND	O_{mz_2}	1	–	32
<i>Acartia</i> feeding preference on zoospore for TOX-A	O_{mz_2}	0.2	–	32
<i>Acartia</i> feeding preference on microzooplankton for Exp5	O_{zz_2}	0	–	32
<i>Acartia</i> feeding preference on microzooplankton for Exp6	O_{zz_2}	1	–	32
<i>Acartia</i> feeding preference on detritus	O_{dz_2}	1	–	32
<i>Acartia</i> grazing threshold on diatom	TH_{pz_2}	0 (off)	$\mu\text{M N}$	10
<i>Acartia</i> grazing threshold on cryptophyte	$\text{TH}_{p_2z_2}$	0 (off)	$\mu\text{M N}$	10

Table 1 (Continued)

Description	Symbol	Value	Units	Source
<i>Acartia</i> grazing threshold on zoospore	TH _{mz2}	0 (off)	μM N	10
<i>Acartia</i> grazing threshold on microzooplankton	TH _{zz2}	0 (off)	μM N	10
<i>Acartia</i> grazing threshold on detritus	TH _{dz2}	0 (off)	μM N	10
Detritus (D)				
Detritus concentration	D	0	μM N	1
Partitioning parameter for mass of dying organisms	β	0.5	–	1

1: From Zhang et al. (2003). 2: From Stoecker et al. (2006). The high shear rate of 3 was chosen as a maximum potential value that might be encountered in an estuarine environment like Pocomoke Flats where *Pfiesteria* outbreaks have occurred and also because Stoecker et al. (2006) show experimentally that a shear rate value of 3 has a significant negative impact on *Pfiesteria* feeding and growth rate. 3: From Anderson et al. (2003). 4: Assuming the maximum grazing rate of TOX-A strains is substantially lower (by a factor of 3) than for NON-IND strains, based upon Burkholder et al. (1997). 5: From Zhang et al. (2003) and also assuming that assimilation efficiency for grazing by zoospores, microzooplankton and *Acartia* is the same for all living food sources. 6: Following Hood et al. (2001), i.e., assuming that DON assimilation is done with 100% efficiency. 7: Following Zhang et al. (2003) and also assuming that the active zooplankton excretion efficiency is the same for all food sources. 8: Assuming that cryptophytes and DON are the most desirable food sources and that they are consumed with equal preference. In contrast, diatoms are considered to be a less palatable food source due to their relatively large size, which is consistent with the feeding behavior studies of Glasgow et al. (1998) and Burkholder et al. (1995). 9: Assuming NON-IND strains do not consume DON. See justification and citations in Section 2.1. 10: In all batch culture simulations presented in this paper it is assumed that all grazing continues on all food sources even if food concentrations are low. 11: Following Zhang et al. (2003), which is consistent with measured *P* vs. *I* curves for *Pfiesteria* from Feinstein et al. (2002). 12: Following Glibert et al. (2006), i.e., assuming that the maximum DIN uptake rate is similar to that of the cryptophyte prey, but that *Pfiesteria*'s affinity for inorganic nitrogen forms such as NO₃ and NH₄ is relatively low. 13: Assuming the TOX-A functional type does not consume DIN. See justification and citations in Section 2.1. 14: Following McCreary et al. (1996) and assuming that *P* in their model represents diatoms. 15: Approximately from Hood et al. (1991), for a near-surface coastal diatom community. 16: For the simulations presented in this paper, dark uptake of nutrients by diatoms and cryptophytes was assumed to be negligible. 17: See discussion in Section 2.2. 18: Following Hood et al. (2001) the fraction of fixed *N* lost to exudation is assumed to be relatively high, in this case 20% of the total fixation per time step. See also Bronk et al. (1996) and references therein. 19: Assuming (arbitrarily) that the initial cryptophyte and microzooplankton biomass is comparable to that of diatoms. 20: Following Zhang et al. (2003) and assuming that natural mortality for Cryptophytes is similar to phytoplankton/diatoms in general. 21: Using the maximum growth rate for cryptophytes from Anderson et al. (2003) which is comparable to values measured for *Storeatula major* by Adolf et al. (2003). It is further assumed that cryptophyte affinity for DIN uptake is similar to that of diatoms. 22: Derived from measured *P* vs. *I* curves for *Storeatula major* by Adolf et al. (2003). 23: Assuming that the cryptophyte maximum growth rate, uptake kinetics and light saturation characteristics for growth on DON are similar to DIN. 24: Assuming moderately high initial DIN and DON concentrations as might be found in estuarine surface waters in the spring/summer transition. 25: Following Hood et al. (2001), though using a slightly higher value, i.e., assuming that living organic matter is composed primarily of liquid/dissolved matter. 26: Assuming that the remineralization rate of labile DON is similar to that of labile detritus. 27: Following Zhang et al. (2003) and assuming that natural mortality and assimilation and growth efficiency parameters for microzooplankton and zooplankton are similar. See also Hood et al. (2001). 28: The maximum grazing rate for microzooplankton is based upon the experimental results of Stoecker et al. (2002) assuming that the measured instantaneous rates were food saturated. The half saturation constant is set at half the value of derived for *Acartia* on the assumption microzooplankton can feed more efficiently than *Acartia* at low food concentrations. 29: Grazing preferences are specified assuming that cryptophytes, detritus and NON-IND zoospores are preferred food sources. As with zoospore grazing, it is assumed that diatoms are discriminated against due to their large size whereas TOX-A zoospores are discriminated against (apparently due to their toxicity) as observed by Stoecker et al. (2002). 30: Initial *Acartia* (i.e., mesozooplankton) biomass is conservatively assumed to be lower than microzooplankton but still relatively high compared to what is typically observed in estuarine and marine systems. 31: Estimated from measured *Acartia* feeding response curves on NON-IND *Pfiesteria* prey from Roman et al. (2006). Redfield C:N ratios were assumed to convert food concentrations from C to N units. 32: Following Roman et al. (2006) preferences were specified assuming that *Acartia* does not discriminate against NON-IND *Pfiesteria*, but following Mallin (1995) and Burkholder and Glasgow (1995) it is assumed that TOX-A zoospores adversely impact *Acartia* behavior and therefore feeding rate. It is assumed that *Acartia* does not discriminate among the other available food sources.

Table 2

Differences between the modeled NON-IND and TOX-A functional types

	NON-IND zoospores	TOX-A zoospores
Maximum grazing rate	High (5.0 day ⁻¹)	Low (1.7 day ⁻¹)
DIN uptake	Yes (μ _{mm} = 1.42)	No (μ _{mm} = 0)
DON consumption	No (O _{n2m} = 0)	Yes (O _{n2m} = 1)
Growth reduced by turbulence	Yes (S _{rate} = 3.0)	Yes (S _{rate} = 3.0)
Susceptibility to microzooplankton grazing	High (O _{mz} = 1.0)	Low (O _{mz} = 0.2)
Susceptibility to <i>Acartia</i> grazing	High (O _{zz} = 1.0)	Low (O _{zz} = 0.2)

that controls the occurrence of *Pfiesteria* blooms (Burkholder and Glasgow, 1997; Stoecker et al., 2006). Stoecker et al. (2006) ran a set of laboratory experiments to test the effects of small-scale shear on *P. piscicida*. They concluded that higher levels of shear have a significant effect on the growth rates of *Pfiesteria*. Based on their results, we derived an empirical function that modifies the growth rate of *Pfiesteria* as a function of shear rate ($\exp(-0.2038 \times S_{\text{rate}})$), i.e., the grazing rate of *Pfiesteria* is exponentially scaled down when turbulence (shear) increases.

NON-IND *Pfiesteria* digest part of the algal cells and retain the chloroplasts of those cells (Lewitus et al., 1999a). These kleptochloroplasts can apparently retain their functionality for a few days (Lewitus et al., 1999a; Anderson et al., 2002). Therefore NON-IND *Pfiesteria* zoospores not only consume phytoplankton as zooplankton do, but they are believed to also use the photosynthesis of the undigested kleptochloroplasts and take up nitrogen as phytoplankton do when light conditions permit photosynthesis of the undigested kleptochloroplasts to occur (Lewitus et al., 1999a, 2006)

$$\text{UPTAKE}_m = \mu_{\text{mm}} \times \text{LDF}_m \times \text{NDF}_m \times \text{SDF}_m \times M \quad (5)$$

UPTAKE_m is the light (LDF_m), dissolved inorganic nitrogen (NDF_m), and size of zoospores (SDF_m) dependent uptake rate of NON-IND *Pfiesteria*. μ_{mm} is the maximum zoospore specific DIN uptake rate. For simplicity, we assume that the value of μ_{mm} is equal to 0 for TOX-A, i.e., they take up DIN at vanishingly low rates (Glibert et al., 2006). Here also, we can vary the value of μ_{mm} to represent any *Pfiesteria* zoospore strains that are between our idealized TOX-A and NON-IND strains.

Uptake of DIN as a function of substrate concentration (herein termed NDF_m) is a Michaelis–Menten function. At very high substrate levels, diffusion of substrate may also occur (Glibert et al., 2006), but this is assumed negligible here. Uptake of DIN is also assumed to be a light dependent function (herein termed LDF_m), and a size dependent function (herein termed SDF_m)

$$\text{NDF}_m = N / (N + \text{MPK}_s) \quad (6)$$

$$\text{LDF}_m = 1 - e^{-I/I_{K_m}} \quad (7)$$

$$\text{If } M_{\text{size}} > 0.5 \times M_{\text{max}}$$

$$\text{SDF}_m = (M_{\text{size}} - 0.5 \times M_{\text{max}}) / (0.5 \times M_{\text{max}}) \quad (8A)$$

else

$$\text{SDF}_m = 0 \quad (8B)$$

where N is the DIN concentration, MPK_s is the half-saturation constant for zoospore DIN uptake, I is the irradiance, and I_{K_m} is the saturation constant for light absorption of zoospores. M_{size} is the size of zoospores and M_{max} is the maximum size of zoospores. When the size of *Pfiesteria* zoospores reaches the maximum size, zoospores undergo cell division. The model assumes that the consequence of the cell division is that the size of the zoospores decreases to half of the maximum size and the abundance of the zoospores doubles.

It is likely that larger zoospores can store more undigested kleptochloroplasts. We therefore assume that the amount of the undigested kleptochloroplasts is positively related to the body size. We further assume that the size of newly divided zoospores (i.e. $0.5 M_{\text{size}}$) is too small to hold any kleptochloroplasts. Therefore, the photosynthesis of the kleptochloroplasts occurs only when the size of the zoospores is between the newly divided size and the maximum size, and when the light and DIN are available. In addition, it is assumed that zoospores can grow and even divide once (because we set the $\text{SDF}_m = 0$ for newly divided zoospore, NON-IND zoospores can maximally divide only once without grazing) if the size of zoospores is close to M_{max} when food sources are exhausted under favorable light and nutrient conditions.

The portion of food consumed by zoospores that cannot be assimilated is expelled. Based on the origin of food sources, zoospore expulsion rate (EXPULSION_m) can be separated into expulsion from diatoms, cryptophytes, and DON. In this model, the zoospore expulsion rate is assumed to be proportional to the grazing rate of the zoospore

$$\text{EXPULSION}_m = \sum \text{EXPULSION}_{im} \quad (9)$$

$$\text{EXPULSION}_{im} = (1 - \text{AE}_{im}) \times \text{GRAZING}_{im} \quad (10)$$

where EXPULSION_{im} , AE_{im} , and GRAZING_{im} are the expulsion rate, the assimilation efficiency, and the grazing rate for zoospore feeding on diatoms ($i = p$), cryptophytes ($i = p_2$), and DON ($i = n_2$). Since we do not expect any expulsion to be associated with DON consumption, we assign $\text{AE}_{n_2m} = 1$.

In order to model the time dependency of total biomass, individual body size, and abundance of *Pfiesteria* zoospores, we separate the zoospore excretion rate (EXCRETION_m) into the active excretion rate (EXCRETION_a) and basal excretion

rate (EXCRETION_b). Based on the origin of food sources, zoospore active excretion rate can be separated into excretion due to cryptophyte versus other phytoplankton (as diatoms) consumption. We assume that the active excretion rate is proportional to the grazing rate of zoospores

$$\text{EXCRETION}_m = \text{EXCRETION}_a + \text{EXCRETION}_b \quad (11)$$

$$\text{EXCRETION}_a = \sum \text{EXCRETION}_{im} \quad (12)$$

$$\text{EXCRETION}_{im} = \text{AEX}_{im} \times \text{GRAZING}_{im} \quad (13)$$

where EXCRETION_{im}, AEX_{im}, and GRAZING_{im} are the active excretion rate, the active excretion efficiency, and the grazing rate for zoospores feeding on diatoms ($i = p$), cryptophytes ($i = p_2$), and DON ($i = n_2$), respectively. In contrast, the basal excretion rate is independent of the grazing rate of zoospores. The basal excretion rate for NON-IND is proportional to zoospore biomass (NON-IND kleptoplast effect was incorporated in the UPTAKE_m function)

$$\text{EXCRETION}_b = \text{BEX}_m \times M \quad (14)$$

where BEX_m is the weight specific basal excretion rate of zoospores.

In this model, microzooplankton and *Acartia* graze on zoospores. GRAZING_{mz} and GRAZING_{mz2} are the microzooplankton and *Acartia* grazing rates in terms of zoospore biomass. The specific formulations are defined in the microzooplankton and *Acartia* equations below.

MORTALITY_m is the zoospore mortality rate in term of biomass. We assume that natural mortality rate of zoospores is proportional to zoospore biomass, and that the specific mortality rate (S_m) is dependent on the size of zoospores and the food availability.

$$\text{if } M_{\text{size}} \leq M_{\text{cri}} \text{ and } dM_{\text{size}}/dt < 0$$

$$S_m = \text{zoospore specific starvation mortality rate} \quad (15A)$$

else

$$S_m = \text{zoospore specific mortality rate} \quad (15B)$$

$$\text{MORTALITY}_m = S_m \times M \quad (16)$$

where M_{cri} is the critical zoospore size.

The rate of change of zoospore abundance (M_{num}) reflects the balance between zoospore division and losses through natural mortality, microzooplankton and

Acartia grazing

$$\begin{aligned} dM_{\text{num}}/dt = & \text{DIVISION}_m - \text{MORTALITY}_{m-\text{num}} \\ & - \text{GRAZING}_{mz-\text{num}} - \text{GRAZING}_{mz2-\text{num}} \end{aligned} \quad (17)$$

DIVISION_m is the zoospore division rate. When the amount of nitrogen assimilated is larger than the metabolic nitrogen losses, the size of the *Pfiesteria* zoospores increases. As described above, when the size of *Pfiesteria* zoospores reaches a maximum size (M_{max}), they undergo cell division. The consequence of the cell division is that the size of the zoospores decreases to half of the maximum size and the abundance of the zoospores doubles.

$$\text{if } M_{\text{size}} \geq M_{\text{max}}$$

$$M_{\text{size}} = M_{\text{size}}/2 \quad \text{and} \quad M_{\text{num}} = M_{\text{num}} \times 2 \quad (18)$$

MORTALITY_{m-num} is the zoospore mortality rate in term of abundance.

$$\text{if } M_{\text{size}} \leq M_{\text{cri}} \text{ and } dM_{\text{size}}/dt < 0$$

$$S_m = \text{zoospore specific starvation mortality rate} \quad (19A)$$

else

$$S_m = \text{zoospore specific mortality rate} \quad (19B)$$

$$\text{MORTALITY}_{m-\text{num}} = S_m \times M_{\text{num}} \quad (20)$$

The microzooplankton and *Acartia* grazing rates in term of zoospore abundance can be calculated from their mass-based grazing rates by dividing by the zoospore size

$$\text{GRAZING}_{mz-\text{num}} = \text{GRAZING}_{mz}/M_{\text{size}} \quad (21)$$

$$\text{GRAZING}_{mz2-\text{num}} = \text{GRAZING}_{mz2}/M_{\text{size}} \quad (22)$$

The size of zoospores at any given time can be calculated from

$$M_{\text{size}} = M/M_{\text{num}} \quad (23)$$

2.2. Diatoms

The rate of change of diatom biomass (P) reflects the balance between DIN (N) uptake and losses through exudation, grazing, and mortality

$$\begin{aligned} dP/dt = & \text{UPTAKE}_p - \text{EXUDATION}_p \\ & - \text{GRAZING}_{pm} - \text{GRAZING}_{pz} \\ & - \text{GRAZING}_{pz2} - \text{MORTALITY}_p \end{aligned} \quad (24)$$

UPTAKE_p is the light and DIN-dependent uptake rate of the diatom. In this model, we assume that diatoms only take up DIN (and not DON) and that they do so at different rates in the light and in the dark

$$\text{UPTAKE}_p = ((\mu_{mp} - \mu_{mpd} \times \text{NDF}_{pd}) \times \text{LDF}_p + \mu_{mpd} \times \text{NDF}_{pd}) \times \text{NDF}_p \times P \quad (25)$$

μ_{mp} is the maximum diatom specific DIN uptake rate, μ_{mpd} is the maximum diatom specific DIN uptake rate in the dark, NDF_{pd} and NDF_p are Michaelis–Menten functions, and LDF_p is a light dependent function. For this purpose, non-saturable uptake of DIN by diatoms, as has been observed under high NO_3^- conditions, is ignored (e.g. Lomas and Glibert, 1999; Collos et al., 1997)

$$\text{NDF}_{pd} = 1 - N/(N + \text{PK}_{sd}) \quad (26)$$

$$\text{NDF}_p = N/(N + \text{PK}_s) \quad (27)$$

$$\text{LDF}_p = 1 - e^{-I/I_{kp}} \quad (28)$$

PK_{sd} is the half-saturation constant for diatom DIN dark uptake, PK_s is the half-saturation constant for diatom DIN light uptake, and I_{kp} is the saturation constant for light absorption.

Mathematically, $\mu_{mpd} \times \text{NDF}_{pd}$ represents the y-intercept of the relationship between diatom DIN uptake rate and irradiance for a given DIN concentration. Diatom dark uptake rate reaches a maximum (μ_{mpd}) at low ambient nutrient concentrations and it goes to zero at very high ambient nutrient concentrations, which is consistent with laboratory and field observations (Cochlan et al., 1991). Although the ratio of the dark uptake rate and the light uptake rate tends to be higher in the nutrient deplete environments compared to nutrient replete environments (Cochlan et al., 1991), for simplicity we assume the value of PK_{sd} equals to one half of PK_s at all times.

Diatoms are also assumed to exude DON (Bronk et al., 1996; Lomas and Glibert, 1999). Exudation of other forms of N (such as NO_2^- and NH_4^+) are ignored for this purpose (Lomas et al., 2000). This exudation is formulated using a simple linear DON exudation rate (EXUDATION_p)

$$\text{EXUDATION}_p = \alpha \times \text{UPTAKE}_p \quad (29)$$

where α is the exuded fraction.

Finally, we also include a simple, linear natural mortality term (MORTALITY_p) in the diatom equation

$$\text{MORTALITY}_p = S_p \times P \quad (30)$$

where S_p is the diatom specific mortality rate.

2.3. Cryptophytes

The rate of change of cryptophyte biomass (P_2) reflects the balance between nitrogen uptake, and losses through grazing, and mortality

$$\begin{aligned} dP_2/dt = & \text{UPTAKE}_{np_2} + \text{UPTAKE}_{n_2p_2} \\ & - \text{GRAZING}_{p_2m} - \text{GRAZING}_{p_2z} \\ & - \text{GRAZING}_{p_2z_2} - \text{MORTALITY}_{p_2} \end{aligned} \quad (31)$$

UPTAKE_{np_2} is the light and concentration dependent uptake rate of DIN. As with diatoms, we differentiate between DIN uptake in the light and in the dark

$$\begin{aligned} \text{UPTAKE}_{np_2} = & ((\mu_{mnp_2} - \mu_{mnp_2d} \times \text{NDF}_{p_2d}) \\ & \times \text{LDF}_{np_2} + \mu_{mnp_2d} \\ & \times \text{NDF}_{p_2d}) \times \text{NDF}_{p_2} \times P_2 \end{aligned} \quad (32)$$

Here, μ_{mnp_2} is the maximum cryptophyte specific DIN uptake rate in the light, μ_{mnp_2d} is the maximum cryptophyte specific DIN uptake rate in the dark, and NDF_{p_2} and NDF_{p_2d} are Michaelis–Menten functions for DIN uptake in the light and dark, respectively. LDF_{np_2} is a light dependent function for cryptophyte DIN uptake

$$\text{NDF}_{p_2d} = 1 - N/(N + P_2K_{snd}) \quad (33)$$

$$\text{NDF}_{p_2} = N/(N + P_2K_{sn}) \quad (34)$$

$$\text{LDF}_{np_2} = 1 - e^{-I/I_{knp_2}} \quad (35)$$

P_2K_{snd} is the half-saturation constant for cryptophyte DIN uptake in the dark, P_2K_{sn} is the half-saturation constant for cryptophyte DIN uptake in the light, and I_{knp_2} is the saturation constant for light absorption for cryptophyte for DIN uptake.

Cryptophytes can assimilate DIN (N) and DON (N_2) (e.g. Berg et al., 2003). In the model we assume that DIN inhibits DON uptake in the same way that NH_4^+ inhibits NO_3^- uptake, although experimental data to verify this for cryptophytes are not available. The uptake of DON ($\text{UPTAKE}_{n_2p_2}$) is similarly assumed to be light and concentration dependent

$$\begin{aligned} \text{UPTAKE}_{n_2p_2} = & ((\mu_{mn_2p_2} - \mu_{mn_2p_2d} \times \text{N}_2\text{DF}_{p_2d}) \\ & \times \text{LDF}_{n_2p_2} + \mu_{mn_2p_2d} \times \text{N}_2\text{DF}_{p_2d}) \\ & \times \text{NDF}_{p_2} \times \text{N}_2\text{DF}_{p_2} \times P_2 \end{aligned} \quad (36)$$

where $\mu_{mn_2p_2}$ is the maximum cryptophyte specific DON uptake rate in the light, $\mu_{mn_2p_2d}$ is the maximum cryptophyte specific DON uptake rate in the dark, and $\text{N}_2\text{DF}_{p_2}$ and $\text{N}_2\text{DF}_{p_2d}$ are DON-dependent Michaelis–Menten functions for uptake in the light and dark, respectively. $\text{N}_2\text{DF}_{p_2}$ is a DIN-dependent function that

imposes an exponential decrease on the DON uptake rate with increasing DIN concentration. $LDF_{n_2p_2}$ is a light dependent function for cryptophyte DON uptake

$$N_2DF_{p_2d} = 1 - N_2/(N_2 + P_2K_{sn_2d}) \quad (37)$$

$$N_2DF_{p_2} = N_2/(N_2 + P_2K_{sn_2}) \quad (38)$$

$$NDF_{p_2} = 1 - N/(N + P_2K_{sn}) \quad (39)$$

$$LDF_{n_2p_2} = 1 - e^{-I/I_{kn_2p_2}} \quad (40)$$

where $P_2K_{sn_2d}$ is the half-saturation constant for cryptophyte DON uptake in the dark, $P_2K_{sn_2}$ is the half-saturation constant for cryptophyte DON uptake in the light, and $I_{kn_2p_2}$ is the saturation constant for light absorption for cryptophyte for DON uptake.

As with diatoms, we include a simple, linear natural mortality term ($MORTALITY_{p_2}$) in the cryptophyte equation

$$MORTALITY_{p_2} = S_{p_2} \times P_2 \quad (41)$$

where S_{p_2} is the cryptophyte specific mortality rate.

2.4. Dissolved inorganic nitrogen

The sources of DIN are assumed to come from excretions and detrital remineralization. Inasmuch as the model represents a closed system, anthropogenic sources of DIN are ignored. The sinks of DIN are diatom, cryptophyte, and NON-IND zoospore uptake. The rate of change of DIN (N) is expressed as

$$\begin{aligned} dN/dt = & \gamma_m \times EXCRETION_m + \gamma_z \times EXCRETION_z \\ & + \gamma_{z_2} \times EXCRETION_{z_2} \\ & + REMINERALIZATION \\ & + REMINERALIZATION_{DON} \\ & - UPTAKE_p - UPTAKE_{np_2} - UPTAKE_m \end{aligned} \quad (42)$$

where γ_m , γ_z , and γ_{z_2} are partitioning parameters of excretions for zoospore, microzooplankton, and *Acartia*. These parameters determine the proportion of the excretion that ends up in DIN.

We assume that detritus exhibits a linear rate of remineralization

$$REMINERALIZATION = \varepsilon \times E \quad (43)$$

where ε is detritus specific remineralization rate.

2.5. Dissolved organic nitrogen

The sources of DON are assumed to come from excretions, diatom exudation and direct release of DON from dying organisms. As for DIN, anthropogenic sources of DON are ignored in the model. The sinks of DON are remineralization, cryptophyte uptake TOX-A *Pfiesteria* zoospore consumption. The rate of change of DON concentration (N_2) is expressed as

$$\begin{aligned} dN_2/dt = & (1 - \gamma_m) \times EXCRETION_m \\ & + (1 - \gamma_z)EXCRETION_z + (1 - \gamma_{z_2}) \\ & \times EXCRETION_{z_2} + EXUDATION_p \\ & + (1 - \beta) \times (MORTALITY_p \\ & + MORTALITY_{p_2} + MORTALITY_m \\ & + MORTALITY_z + MORTALITY_{z_2}) \\ & - REMINERALIZATION_{DON} - UPTAKE_{n_2p_2} \\ & - GRAZING_{n_2m} \end{aligned} \quad (44)$$

As with DIN, DON is remineralized using a simple linear form

$$REMINERALIZATION_{don} = \varepsilon_2 \times N_2 \quad (45)$$

where ε_2 is DON specific remineralization rate.

We specify direct release of DON from dying diatoms, cryptophytes, zoospores, microzooplankton, and *Acartia* using the partitioning parameter (β), which determines the proportion of the mass of the dying organisms that ends up in the detritus pool.

2.6. Microzooplankton

The rate of change of microzooplankton biomass (Z) reflects the balance between the gain through omnivorous grazing and losses through defecations, excretions, *Acartia* grazing, and natural mortality

$$\begin{aligned} dZ/dt = & GRAZING_z - DEFECATION_z \\ & - EXCRETION_z - GRAZING_{zz_2} \\ & - MORTALITY_z \end{aligned} \quad (46)$$

As with the zoospores, a saturating hyperbolic expression is used to define the grazing rate of microzooplankton ($GRAZING_z$). We assume that microzooplankton graze on diatoms, cryptophytes, zoospores, and detritus. We also allow a grazing threshold for each food source (i)

$$GRAZING_z = \sum GRAZING_{iz} \quad (47)$$

If $i \leq TH_{iz}$

$$GRAZING_{iz} = 0 \quad (48A)$$

else

$$GRAZING_{iz} = (G_{mz} \times i \times O_{iz} \times Z) / THETA_z \quad (48B)$$

$$THETA_z = O_{pz} \times P + O_{p_2z} \times P_2 + O_{mz} \times M + O_{dz} \times D + ZK_s \quad (49)$$

$GRAZING_{iz}$, TH_{iz} , and O_{iz} are the grazing rate, grazing threshold, and the grazing preference (which scales from 0 to 1) for microzooplankton feeding on diatoms ($i = p$), cryptophytes ($i = p_2$), zoospores ($i = m$), and detritus ($i = d$), respectively. G_{mz} is the maximum specific rate for microzooplankton grazing, and ZK_s is the half-saturation constant for microzooplankton grazing.

The portion of food consumed by microzooplankton that cannot be assimilated is defecated. Based on the origin of food sources, the microzooplankton defecation rate ($DEFECATION_z$) can be separated into defecation from diatoms, cryptophytes, zoospores, and detritus

$$DEFECATION_z = \sum DEFECATION_{iz} \quad (50)$$

$$DEFECATION_{iz} = (1 - AE_{iz}) \times GRAZING_{iz} \quad (51)$$

$DEFECATION_{iz}$, AE_{iz} , and $GRAZING_{iz}$ are the defecation rate, the assimilation efficiency, and the grazing rate for microzooplankton feeding on diatoms ($i = p$), cryptophytes ($i = p_2$), zoospores ($i = m$), and detritus ($i = d$).

For simplicity, we do not differentiate basal excretion and the active excretion for microzooplankton. Microzooplankton excretion ($EXCRETION_z$) can also be separated into excretion from diatoms, cryptophytes, zoospores, and detritus

$$EXCRETION_z = \sum EXCRETION_{iz} \quad (52)$$

$$EXCRETION_{iz} = (AE_{iz} - GE_{iz}) \times GRAZING_{iz} \quad (53)$$

$EXCRETION_{iz}$, AE_{iz} , and GE_{iz} are the excretion rate, the assimilation efficiency, and the growth efficiency for microzooplankton feeding on diatoms ($i = p$), cryptophytes ($i = p_2$), zoospores ($i = m$), and detritus ($i = d$).

Finally, we assume that the natural mortality rate of microzooplankton is proportional to microzooplankton biomass

$$MORTALITY_z = S_z \times Z \quad (54)$$

S_z is the specific mortality rate of the microzooplankton.

2.7. *Acartia*

The rate of change of *Acartia* biomass (Z_2) reflects the balance between the gain through omnivorous grazing and losses through defecations, excretions, and natural mortality

$$\frac{dZ_2}{dt} = GRAZING_{z_2} - DEFECATION_{z_2} - EXCRETION_{z_2} - MORTALITY_{z_2} \quad (55)$$

As in previous grazing expressions, a saturating hyperbolic function is used to define the grazing rate of *Acartia* ($GRAZING_{z_2}$). We assume that *Acartia* graze on diatoms, cryptophytes, zoospores, detritus, and microzooplankton, and again we set a grazing threshold for each food source

$$GRAZING_{z_2} = \sum GRAZING_{iz_2} \quad (56)$$

If $i \leq TH_{iz_2}$

$$GRAZING_{iz_2} = 0 \quad (57A)$$

else

$$GRAZING_{iz_2} = (G_{mz_2} \times i \times O_{iz_2} \times Z_2) / THETA_{z_2} \quad (57B)$$

$$THETA_{z_2} = O_{pz_2} \times P + O_{p_2z_2} \times P_2 + Omz_2 \times M + O_{dz_2} \times D + O_{zz_2} \times Z + Z_2K_s \quad (58)$$

$GRAZING_{iz_2}$, TH_{iz_2} , and O_{iz_2} are the grazing rate, grazing threshold, and the grazing preference for *Acartia* feeding on diatoms ($i = p$), cryptophytes ($i = p_2$), zoospores ($i = m$), detritus ($i = d$), and microzooplankton ($i = z$), respectively. G_{mz_2} is the maximum specific rate for *Acartia* grazing, and Z_2K_s is the half-saturation constant for *Acartia* grazing.

As with microzooplankton, *Acartia* defecation rate ($DEFECATION_{z_2}$) can be separated according to these food sources designated by the indexes (i) defined above

$$DEFECATION_{z_2} = \sum DEFECATION_{iz_2} \quad (59)$$

$$DEFECATION_{iz_2} = (1 - AE_{iz_2}) \times GRAZING_{iz_2} \quad (60)$$

$DEFECATION_{iz_2}$, AE_{iz_2} , and $GRAZING_{iz_2}$ are defined as they are for microzooplankton except using the specific *Acartia* food sources.

Similarly, *Acartia* excretion ($EXCRETION_{z_2}$) can be separated into excretion from the different food sources, and we do not differentiate basal and active

excretion

$$\text{EXCRETION}_{z_2} = \sum \text{EXCERITION}_{iz_2} \quad (61)$$

$$\text{EXCRETION}_{iz_2} = (\text{AE}_{iz_2} - \text{GE}_{iz_2}) \times \text{GRAZING}_{iz_2} \quad (62)$$

with EXCRETION_{iz_2} , AE_{iz_2} , and GE_{iz_2} defined as above using *Acartia* food sources. The natural mortality rate of *Acartia* is also assumed to be proportional to *Acartia* biomass, with the specific mortality rate S_{z_2}

$$\text{MORTALITY}_{z_2} = S_{z_2} \times Z_2 \quad (63)$$

2.8. Detritus

The sources of detritus (D) are assumed to come from zoospore expulsion, microzooplankton defecation, *Acartia* defecation and dead bodies of organisms. The latter is divided between detritus and DON using the partitioning parameter, β . The sinks of the detritus pool are grazing and remineralization (defined above). The rate of change of detritus concentration is expressed as

$$\begin{aligned} dD/dt = & \text{EXPULSION}_m + \text{DEFECATION}_z \\ & + \text{DEFECATION}_{z_2} + \beta \times (\text{MORTALITY}_p \\ & + \text{MORTALITY}_{p_2} + \text{MORTALITY}_m \\ & + \text{MORTALITY}_z + \text{MORTALITY}_{z_2}) \\ & - \text{GRAZING}_{dz} - \text{GRAZING}_{dz_2} \\ & - \text{REMINERALIZATION} \end{aligned} \quad (64)$$

3. Results and discussion

Using this generic model, we carried out six modeling “experiments”. These experiments are intended to emulate typical batch-culture laboratory experiments, i.e., with the modeled culture initialized with relatively low *Pfiesteria* concentrations and then the population is allowed to grow over a period of 10 days under different turbulence, nutrient and grazing conditions, but with a constant 12-h light and 12-h dark cycle in all model runs. The effect on growth of both NON-IND and TOX-A functional types of *Pfiesteria* was determined in separate experiments, i.e., *Pfiesteria* was either parameterized as the NON-IND or TOX-A form in each of the runs described below. Through these various experiments our goal was collectively to provide answers to the following questions: (1) What is the effect of turbulence on *Pfiesteria* population dynamics? (2) What are the differences in the

population dynamics of TOX-A and NON-IND functional type of *Pfiesteria*? (3) What conditions give rise to dominance of one functional type versus the other? (4) What are the effects of different nutrient concentrations and DIN/DON ratios on *Pfiesteria* population dynamics? and (5) How does top-down control by microzooplankton and *Acartia* grazing impact *Pfiesteria* abundance?

3.1. First experiment (low turbulence and high DIN:DON ratio)

In our first model experiment we subjected our hypothetical NON-IND and TOX-A model cultures of *Pfiesteria* to low levels of turbulence ($S_{\text{rate}} = 0$, Table 1, i.e., equivalent to those that might be found in a stratified estuarine environment), a high initial DIN/DON ratio (=5), but effects of microzooplankton and *Acartia* grazing were excluded (Fig. 2). Over a 4 days time interval, the biomass of diatoms was greatly reduced and cryptophyte biomass was exhausted by NON-IND *Pfiesteria*. Zoospore biomass reached a maximum by day 4 and then declined due to food limitation even though there was finite diatom biomass due to the low preference for diatom feeding (Fig. 2A, Table 1). The concentration of DIN declined sharply over the first 2 days but then began to recover after the biomass (uptake) of the diatoms and cryptophytes was diminished (Fig. 2A). DON concentrations increased over the course of the experiment due to reduced cryptophyte biomass (uptake) and absence of DON consumption by NON-IND *Pfiesteria*.

In contrast, the TOX-A functional type grew much more slowly over the course of the 10-day experiment and the biomass of diatoms and cryptophytes increased significantly after initialization, which depleted DIN concentrations faster and to lower levels (Fig. 2B). The diatom biomass reached a maximum before day 2 and then began to decline whereas the cryptophytes reached a maximum 1–2 days later and then declined. In both cases the declines were due to a combination of nutrient depletion and grazing losses imposed by *Pfiesteria*. Both DIN and DON concentrations were substantially reduced by the end of the experiment due to the relatively high biomass of diatoms and cryptophytes and also uptake of DON by TOX-A *Pfiesteria* (Fig. 2B).

NON-IND zoospores divided at a faster rate than did those of the TOX-A functional type (Fig. 2C and D) because they have a higher maximum zoospore specific grazing rate (Table 1) and also benefit from DIN uptake, which enhances their assimilation efficiency. After cell division, the abundance of *Pfiesteria* zoospores doubled

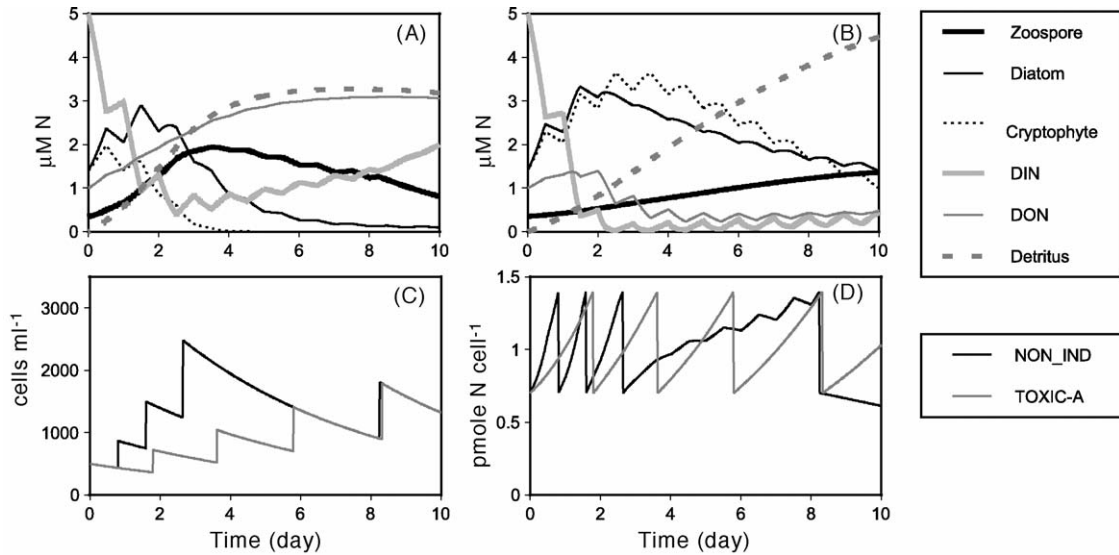


Fig. 2. First modeling experiment (low turbulence and high DIN:DON ratio). *Pfiesteria* zoospore biomass, diatom biomass, and cryptophyte biomass, DIN concentration, DON concentration, and detritus concentration vs. time for NON-IND (A) and TOX-A (B). *Pfiesteria* zoospore abundance vs. time (C). *Pfiesteria* zoospore size vs. time (D).

(Fig. 2C) and the size of *Pfiesteria* zoospores was reduced to half (Fig. 2D). Note also the long decline in the size of the NON-IND zoospores after food limitation sets in after day 4, which did not happen with the TOX-A functional type (Fig. 2D).

This experiment shows that, in the absence of top-down control, our modeled NON-IND functional type grew faster than TOX-A under high DIN and low DON conditions when turbulence was low, and the NON-IND functional type was able to more rapidly crop and control its prey (diatoms and cryptophytes). In addition, the NON-IND population clearly declined in both biomass and cell size after its prey was depleted.

These differences between our modeled NON-IND and TOX-A types are generally consistent with observed differences (Burkholder et al., 2001b), e.g., NON-IND functional types attain higher zoospore production when growing on algal prey whereas TOX-A does not. The latter two results are also consistent with grazing experiments that have been carried out by Lin et al. (2004), which show that *Pfiesteria* may control prey populations and that the abundance of appropriate prey may be an important factor regulating *Pfiesteria* abundance in nature. The conditions in this model experiment (low turbulence, high DIN and low grazing pressure) that demonstrated favorable growth of NON-IND functional types, at least until prey were depleted, might be representative of a stratified estuarine environment with high point source NO_3^- loading (e.g., sewage treatment plant) and/or high non-point

source NH_4^+ loading (e.g., fertilizer from farm fields or runoff from intensive animal operations).

3.2. Second experiment (high turbulence and high DIN:DON ratio)

In the second experiment, we simulated the effect of higher turbulence on *Pfiesteria* population dynamics. All terms and conditions are the same as the first experiment except for turbulence parameter. That is, we increased the shear rate (S_{rate}) in Eq. (3B) to a value of 3 (Table 1). This value of S_{rate} might be comparable to the highest values found in the surface mixed layer or the turbulent bottom boundary layer in a shallow estuarine environment (Stoecker et al., 2006). This increase effectively depressed the maximum grazing rate of NON-IND and TOX-A strains by 54%.

Compared to the first experiment, NON-IND zoospores grew slower and biomass did not reach a maximum until after day 6 (Fig. 2A versus Fig. 3A). As a result of this lower grazing rate, the NON-IND strain imposed lower grazing pressure on its diatom and cryptophyte prey, and both DIN and DON concentrations were drawn down to lower levels ($\sim 0 \mu\text{M}$ DIN between days 2 and 4 and DON $\sim 1\text{--}2 \mu\text{M}$ over the course of the experiment). In contrast, with turbulence imposed TOX-A biomass declined very slowly throughout the run (Fig. 2B versus Fig. 3B), i.e., the net growth rate was slightly negative. Compared to the no-turbulence run, cryptophyte biomass increased more

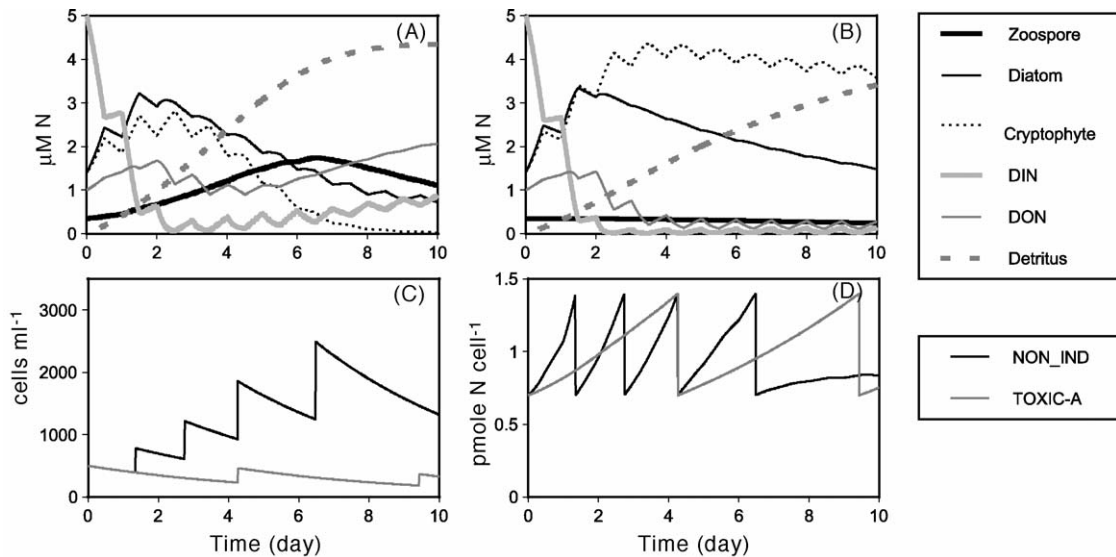


Fig. 3. Second modeling experiment (high turbulence and high DIN:DON ratio). All terms and conditions are same as the first experiment except for the higher turbulence. *Pfiesteria* zoospore biomass, diatom biomass, and cryptophyte biomass, DIN concentration, DON concentration, and detritus concentration vs. time for NON-IND (A) and TOX-A (B). *Pfiesteria* zoospore abundance vs. time (C). *Pfiesteria* zoospore size vs. time (D).

due to the reduced *Pfiesteria* grazing pressure and remained higher throughout the experiment, whereas the diatom biomass was relatively unchanged (Fig. 2B versus Fig. 3B). The DIN and DON concentrations became more depleted over the course of the run due to increased cryptophyte uptake. Under these more turbulent conditions, the doubling time of the TOX-A functional type was substantially longer than the NON-IND (Fig. 3C and D). Note that the NON-IND functional type continued to divide longer with turbulence because they depleted their prey more slowly (Fig. 2C versus Fig. 3C).

The lowering of *Pfiesteria* grazing due to increased turbulence, as demonstrated by Stoecker et al. (2006), presumably happens because turbulence reduces prey capture success. This effect has also been demonstrated with larval fish when turbulence levels get too high (Fiksen and MacKenzie, 2002). Although the Stoecker et al. (2006) study was conducted only with NON-IND zoospores, it is reasonable to assume (as we have done here) that turbulence has a detrimental effect on grazing by TOX-A zoospores as well. We note, however, that Eq. (3B) also specifies that DON uptake by TOX-A strains is reduced when turbulence levels are increased. We know of no experimental evidence to either confirm or deny this assumption. It is entirely possible that increased turbulence actually increases the DON consumption rate of *Pfiesteria* because it would tend to increase the rate of DON diffusion to the cell surface.

In general, these model results suggest that turbulent environments would tend to favor NON-IND strains over TOX-A functional types of *Pfiesteria* when DIN/DON ratios are high, for essentially the same reasons that were noted above. That is, because NON-IND zoospores divide at a faster rate than those of the TOX-A functional type because they have a higher maximum zoospore specific grazing rate (Table 1) and also benefit from DIN uptake, which enhances their assimilation efficiency. These differences in the growth rate of the two strains are simply exacerbated when turbulence levels are high.

3.3. Third experiment (low turbulence and low DIN:DON ratio)

In the third experiment, we simulated the effect of nutrient concentration and composition on *Pfiesteria* population dynamics. All terms and conditions are same as the first experiment except for a change of nutrient concentrations from the previously high DIN and low DON condition to a low DIN and high DON condition. Specifically, we lowered the DIN/DON ratio from 5 to 0.2 while keeping the total DIN + DON concentration the same ($=6 \mu\text{M}$).

Compared to the first experiment, NON-IND zoospore biomass reached a lower maximum between days 3 and 4 (Fig. 2A versus Fig. 4A) and the diatom and cryptophyte prey were depleted a little more slowly. This happens because the lower DIN concentrations

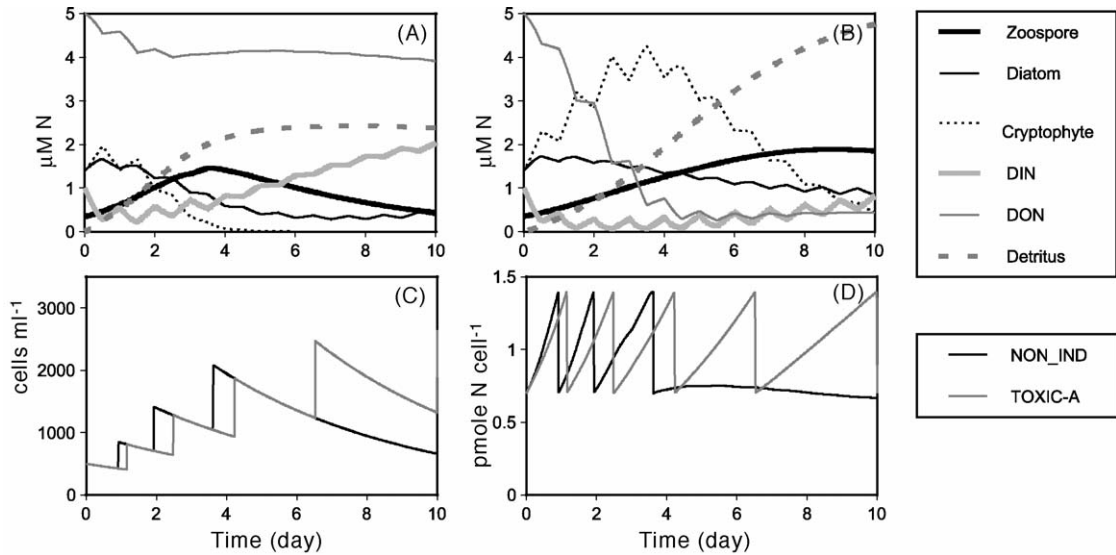


Fig. 4. Third modeling experiment (low turbulence and low DIN:DON ratio). All terms and conditions are same as the first experiment except for the change of nutrient condition from the high DIN and low DON to the low DIN and high DON. *Pfiesteria* zoospore biomass, diatom biomass, and cryptophyte biomass, DIN concentration, DON concentration, and detritus concentration vs. time for NON-IND (A) and TOX-A (B). *Pfiesteria* zoospore abundance vs. time (C). *Pfiesteria* zoospore size vs. time (D).

restrict the growth of the NON-IND strain. Note that the lower DIN also restricts the diatom growth, which increases less in the beginning of the experiment. Concentrations of DIN declined initially but then increased over the course of the experiment as DON and particulate matter was remineralized. This DIN was not utilized because the diatoms and cryptophytes were substantially depleted by *Pfiesteria*. And without their preferred prey as a source of kleptochloroplastids, *Pfiesteria* were unable to effectively utilize DIN.

In contrast, TOX-A zoospores grew faster because more DON was available which increased their intrinsic rate of growth (Fig. 2B versus Fig. 4B). As a result, they had a more significant impact on their diatom and cryptophyte prey (especially the latter), which were both also more nutrient limited. The cryptophytes declined rapidly after day 4 due to grazing as the *Pfiesteria* population increased. Compared to the NON-IND run, DON concentrations declined much more with TOX-A because it was taken up by cryptophytes and *Pfiesteria*, and DIN concentrations remain relatively constant and low, revealing an approximate balance between uptake by diatoms and cryptophytes versus remineralization associated with *Pfiesteria* grazing. Note that with a high DON/DIN ratio the TOX-A functional type divided almost as fast as the NON-IND type before prey for the latter was depleted. TOX-A also continued to grow over the course of the experiment (Fig. 4C and D).

By way of comparison to natural systems, we might consider that this experiment simulates stratified, DON replete conditions that are found in shallow estuarine tributaries that are subject to farm-associated organic nutrient loading, i.e., either directly from animal egesta and excreta, and/or indirectly through the use of this material as fertilizer. This type of environment can be found, for example, in the shallow tributaries on the eastern shore of Chesapeake Bay, USA, in areas adjacent to chicken farms or fields where chicken excrement is used to fertilize crops (e.g. Glibert et al., 2005c). Similar environments can also be found in shallow tributaries of the Albermarle-Pamlico Sound (North Carolina, USA) where there is intensive pig-farming (e.g., Mallin, 2000a,b). According to our model results, these environments would ultimately favor the growth of the TOX-A functional type of *Pfiesteria* if the conditions remain stable long enough for their biomass to increase and accumulate (i.e., for at least several days).

3.4. Fourth experiment (microzooplankton grazing on *Pfiesteria*)

In the fourth experiment, we introduced the effect of microzooplankton grazing on *Pfiesteria*. All other terms and conditions were the same as the first experiment. Compared to the first experiment, the NON-IND biomass declined rapidly after initialization and became

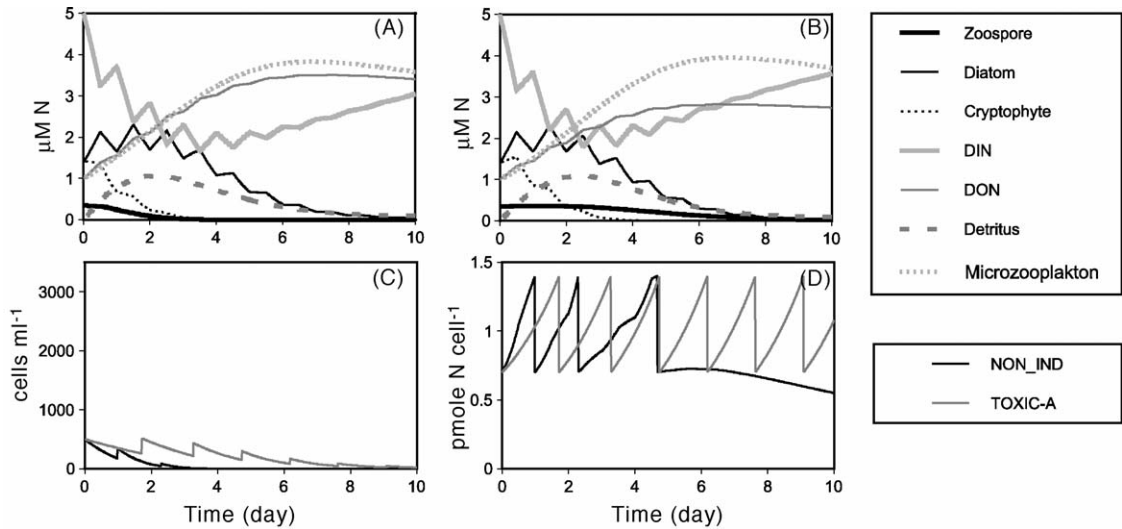


Fig. 5. Fourth modeling experiment (microzooplankton grazing on *Pfiesteria*). All terms and conditions are same as the first experiment except for the addition of microzooplankton grazing. *Pfiesteria* zoospore biomass, diatom biomass, and cryptophyte biomass, DIN concentration, DON concentration, detritus concentration, and microzooplankton biomass vs. time for NON-IND (A) and TOX-A (B). *Pfiesteria* zoospore abundance vs. time (C). *Pfiesteria* zoospore size vs. time (D).

exhausted by day 3 due to the additional losses/mortality associated with direct microzooplankton grazing (Fig. 2A versus Fig. 5A). The cryptophyte prey was driven even more rapidly to depletion than in experiment 1 and the diatoms were also depleted before the end of the run due to the additional microzooplankton grazing losses. The rapid disappearance of *Pfiesteria* and its prey allowed DIN concentrations to remain higher throughout the experiment, i.e., they never dropped much below 2 μM . Microzooplankton increased gradually over the first 6 days of the experiment and then began to decline after their prey became depleted.

The response of the TOX-A zoospores to this added grazing pressure was similar to the response of the NON-IND zoospores but less pronounced because of the reduced preference for grazing on the TOX-A strain (Table 1), i.e., the zoospore population declined over the course of the 10 day experiment along with their diatom and cryptophyte prey due to the microzooplankton grazing losses, while DIN concentrations remained relatively high. Interestingly, even though the zoospore cell numbers declined in both the NON-IND and TOX-A cases due to the added grazing losses (Fig. 5C), and the NON-IND stopped dividing after day 4 due to depletion of the diatom and cryptophyte prey (Fig. 5D), the TOX-A cells continued to grow and divide throughout the 10-day experiment, presumably due to high DON concentrations which supplemented their growth even when prey concentrations were depleted (Fig. 5D).

These model results are generally consistent with laboratory and in situ grazing experiments that have been conducted by Stoecker et al. (2000), Stoecker and Gustafson (2002), and Stoecker et al. (2002), which suggest that *Pfiesteria* zoospore populations can be effectively controlled by microzooplankton grazing. Stoecker and Gustafson (2002) argue that blooms of *Pfiesteria* should only be possible during windows of low grazing pressure. These studies also suggest that microzooplankton grazing impacts on toxic zoospores are less, presumably due to the inhibitory or mortality effects of the toxins, which would imply that toxic strains are more likely to bloom when grazers are present. Our model shows that the TOX-A functional type continues to grow and divide even in the presence of microzooplankton grazing pressure, apparently due to the availability of DON. Furthermore, Glibert et al. (2006) demonstrated that while nitrogen uptake by *Pfiesteria* contributes a small percentage of actively feeding NON-IND cells, it may contribute a significantly higher percentage of total nutrition in TOX-A cells.

3.5. Fifth experiment (*Acartia* grazing on *Pfiesteria*)

In the fifth experiment, we simulated the effect of *Acartia* (mesozooplankton) grazing on *Pfiesteria*. All terms and conditions were the same as the fourth experiment, except for the addition of *Acartia* grazing

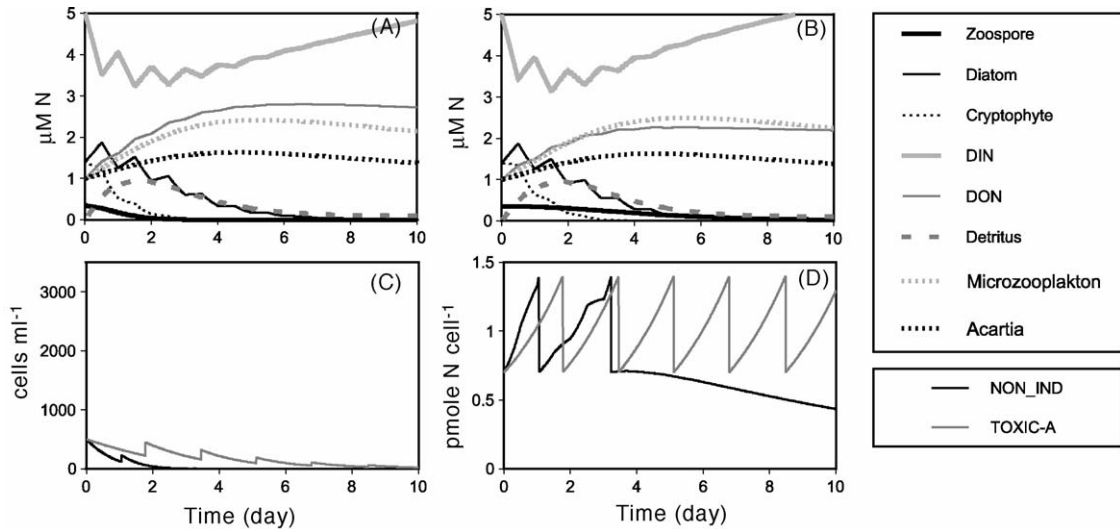


Fig. 6. Fifth modeling experiment (*Acartia* grazing on *Pfiesteria*). All terms and conditions are same as the fourth experiment except for the addition of *Acartia* grazing and the assumption that *Acartia* do not eat microzooplankton. *Pfiesteria* zoospore biomass, diatom biomass, and cryptophyte biomass, DIN concentration, DON concentration, detritus concentration, microzooplankton biomass, *Acartia* biomass vs. time for NON-IND (A) and TOX-A (B). *Pfiesteria* zoospore abundance vs. time (C). *Pfiesteria* zoospore size vs. time (D).

and the assumption that *Acartia* does not eat microzooplankton. A comparison of Figs. 5 and 6 show that the results from experiments with and without *Acartia* grazing imposed are similar. Compared to the fourth experiment, NON-IND biomass declined slightly faster and became exhausted before day 2 (Fig. 5A versus Fig. 6A) due to the slightly greater mortality losses imposed by *Acartia* grazing. The diatom and cryptophyte prey were also consumed slightly faster. The *Acartia* biomass responded much like microzooplankton, i.e., first increasing and then gradually declining after the prey were depleted. DIN concentrations remained even higher throughout the experiment due to the lowering of phytoplankton biomass (uptake).

The response of the TOX-A cells to *Acartia* grazing was similar to the NON-IND cells, i.e., a slightly more rapid decline of zoospores and their prey due to the increased grazing pressure, though the impact on *Pfiesteria* was even smaller because of *Acartia*'s reduced preference for grazing on the TOX-A functional type. Note that zoospore cell concentrations were lowered only a small amount with *Acartia* grazing added (Fig. 6C). However, both the NON-IND and TOX-A zoospores took longer to divide presumably due to the more rapid depletion of their prey (Fig. 6C and D). As in the fourth experiment, the TOX-A cells continued to grow and divide throughout the experiment by consuming DON whereas the NON-IND functional type stopped growing after only two divisions due to prey depletion (Fig. 6D).

Roman et al. (2006) demonstrated that *Acartia tonsa* grazes on zoospore stages of non-inducible and potentially weakly toxic strains of *Pfiesteria*, that the ingestion rate of *Pfiesteria* exhibits a hyperbolic (saturating) feeding response, and that *Acartia* grazes on *Pfiesteria* at rates that are comparable to similar sized phytoplankton species. With the exception of the latter, all of these results are consistent with our model formulation. In our model we chose to reduce the grazing preference on the TOX-A functional type (as we did with microzooplankton) because *Acartia* has been observed to exhibit erratic behavior in short term (3-day) feeding experiments with toxic *Pfiesteria* (Burkholder and Glasgow, 1995; Mallin, 1995). If it is assumed that *Acartia* consumes TOX-A with equal preference to its other food sources (as with the NON-IND functional type), then its impact on the *Pfiesteria* population is more significant, but still not nearly as large as that of microzooplankton (results not shown).

Roman et al. (2006) concluded that significant grazing control of *Pfiesteria* by *Acartia* would only occur at very high concentrations (>10 copepods L^{-1}) and that microzooplankton are therefore more likely to exert grazing control in situ. These conclusions are consistent with our model results, i.e., the addition of *Acartia* grazing has a fairly small impact on both NON-IND and TOX-A functional types of *Pfiesteria*, even when relatively high *Acartia* biomass is specified relative to microzooplankton (Table 1).

This happens because *Acartia* has a lower maximum grazing rate and a much higher half-saturation constant for grazing saturation compared to microzooplankton in our model. The *Acartia* grazing parameters were, in fact, derived from Roman et al. (2006). These results therefore appear to confirm the conclusions of Roman et al. (2006) in a dynamic ecosystem context.

3.6. Sixth experiment (*Acartia* grazing on microzooplankton and *Pfiesteria*)

In the final model experiment, we simulated the effect of a trophic cascade (*Acartia* grazing on microzooplankton which, in turn, grazed on *Pfiesteria*). All terms and conditions were the same as the fifth experiment, except for removal of the assumption that *Acartia* do not eat microzooplankton. As a result, the microzooplankton concentrations declined rapidly and were completely eliminated by day 6 in both the NON-IND and TOX-A cases (Fig. 7A and B). Compared to the fifth experiment, NON-IND biomass declined a little more slowly and was not exhausted until day 4 (Fig. 6A versus Fig. 7A) due to the reduced microzooplankton grazing pressure. However, the impact of this change on *Pfiesteria* (and also diatoms and cryptophytes) was relatively modest because *Acartia* grazes directly on the NON-IND functional type, i.e., microzooplankton grazing pressure is reduced but *Acartia* grazing pressure is added.

In contrast, the impact upon the TOX-A functional type of adding *Acartia* grazing on microzooplankton was more pronounced, i.e., instead of declining as in the fifth experiment, *Pfiesteria* increases slightly over the course of the run (Fig. 6B versus Fig. 7B). The diatom and cryptophyte biomasses were relatively unchanged. Thus, at least in the TOX-A case, it appears that a trophic cascade gives rise to a compensatory effect, where *Acartia* grazing reduces microzooplankton biomass and grazing on *Pfiesteria* which, in turn, allows a net positive zoospore population growth rather than decline. It should be noted, however, that this result is critically dependent upon the assumption of a reduced preference for *Acartia* feeding on the TOX-A functional type, i.e., *Acartia* reduced microzooplankton grazing pressure on *Pfiesteria* with no compensatory increase in direct grazing losses from *Acartia*.

In terms of the nutrient concentration effects, Fig. 7 shows that the addition of *Acartia* grazing on microzooplankton results in fairly modest changes in both DIN and DON concentrations because of the compensatory effects of *Acartia* versus microzooplankton grazing, i.e., the autotrophic biomass and uptake were not greatly altered and heterotrophic recycling switched from microzooplankton toward *Acartia*.

We are not aware of any experimental evidence indicating that trophic cascade effects are involved in regulating *Pfiesteria* populations dynamics. Several studies have demonstrated that top-down control can influence phytoplankton concentrations in lakes (see

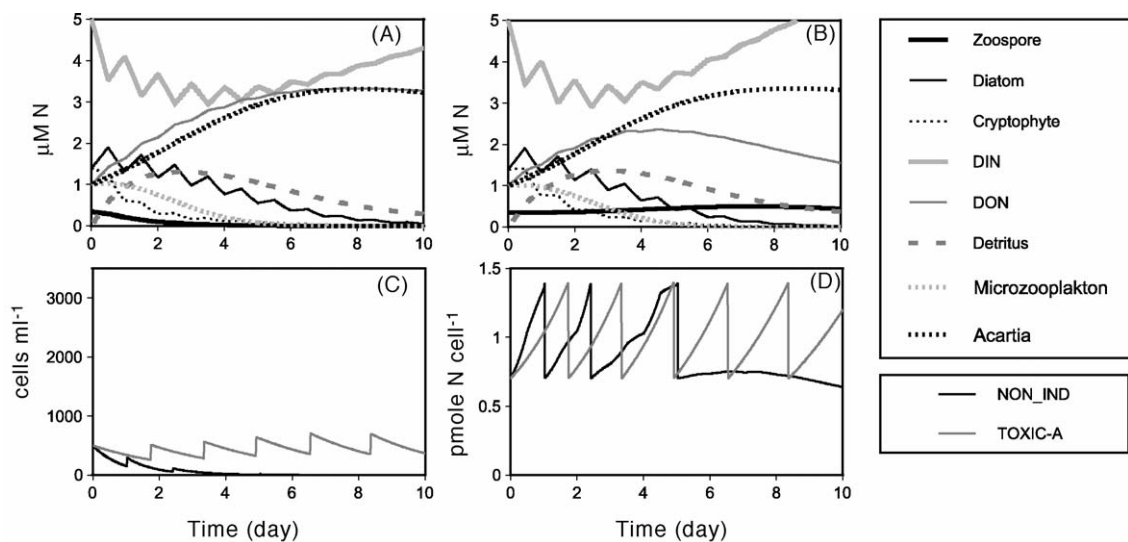


Fig. 7. Sixth modeling experiment (*Acartia* grazing on microzooplankton and *Pfiesteria*). All terms and conditions are same as the fifth experiment except for deletion of the assumption that *Acartia* do not eat microzooplankton. *Pfiesteria* zoospore biomass, diatom biomass, and cryptophyte biomass, DIN concentration, DON concentration, detritus concentration, microzooplankton biomass, *Acartia* biomass vs. time for NON-IND (A) and TOX-A (B). *Pfiesteria* zoospore abundance vs. time (C). *Pfiesteria* zoospore size vs. time (D).

Carpenter et al., 1985 and references therein). Glibert (1998) synthesized the effects of top-down control on plankton nitrogen cycling, and found that the impact of mesozooplankton on rates of nitrogen cycling was complex; on the one hand, they release inorganic and organic nitrogen by excretion and ‘sloppy feeding’, but they also control both the rates of nitrogen regeneration and uptake by grazing the microzooplankton, typically the primary regenerators of inorganic nitrogen, and phytoplankton, the primary consumers of nitrogen. The *Pfiesteria* case is unique, however, in that *Pfiesteria* can serve as both a consumer and potentially a regenerator of nitrogen.

The extent to which trophic cascades are important in regulating population dynamics in marine systems is still an open question (Calbet and Landry, 1999), though evidence is beginning to accumulate that they are (e.g., Feigenbaum and Kelly, 1984; Purcell and Decker, 2005). Suffice it to say, that our model results and the experimental evidence (Stoecker et al., 2000, 2002; Stoecker and Gustafson, 2002; Roman et al., 2006) suggest that direct grazing impacts by microzooplankton are very important in regulating *Pfiesteria* population (and bloom) dynamics and that trophic cascade effects could be important, especially with the TOX-A functional type if the grazers avoid them.

4. Summary and conclusions

In this paper we have described a semi-idealized marine ecosystem model designed as a heuristic tool for exploring the population dynamics of non-inducible versus toxic strains of *Pfiesteria*. This is the first model which simulates differences between non-inducible and toxic strains of *Pfiesteria* in a food web context. Here we summarize the results from this effort as they relate to the five major questions that we posed above.

Toxic and non-inducible strains of *Pfiesteria* differ substantially in terms of what they eat and how they utilize it to optimize their growth. In our model formulation, the NON-IND functional type is an idealized kleptochloroplastidic dinoflagellate that cannot utilize DON directly, whereas the TOX-A functional type is not kleptochloroplastidic but can utilize DON. This model does not fully reflect empirical results in this regard, in that direct uptake of nitrogen has been found by all functional types of *Pfiesteria* (Glibert et al., 2006). However, consistent with empirical data is the fact that organic nitrogen is used preferentially and taken up in a significantly higher proportion by TOX-A cells compared to NON-IND cells (Glibert et al., 2006). According to our model these differences give rise to

very different impacts on prey and nutrient concentrations, but the specific nature of these impacts depends upon the DIN/DON ratio. Regardless of the turbulence levels, under high DIN/DON ratio NON-IND strains grow much faster because they have a higher maximum specific grazing rate and also benefit from DIN uptake. Also, because they grow fast, they have a much more significant impact on their prey. However, when DON concentrations are elevated relative to DIN, this advantage is much less because DON consumption boosts the growth rate of the TOX-A cells. According to our model, grazing effects should not fundamentally alter these conclusions. However, grazing losses may confer additional advantage to the TOX-A functional type if grazing rates are reduced on toxic cells, which is consistent with microzooplankton grazing studies (Stoecker et al., 2000, 2002; Stoecker and Gustafson, 2002).

We already know from Stoecker et al. (2006) that the grazing rate of non-toxic strains of *Pfiesteria* is diminished as turbulence levels increase. We have incorporated a parameterization into our model to reproduce this effect. Although the impact of turbulence upon the growth rate of NON-IND and TOX-A functional types is the same in our model, we found that increased turbulence is more detrimental to the latter because it grows more slowly, giving rise to a net negative growth rate. Overall, these results suggest that turbulent conditions will tend to favor non-toxic strains of *Pfiesteria* which can still increase under turbulent conditions. However, we must keep in mind that turbulence can also impact the feeding rate of microzooplankton and mesozooplankton grazers. Fish larvae feeding models (e.g., Fiksen and MacKenzie, 2002) suggest that as turbulence increases, feeding rates tend to first increase due to increased encounter rates, but then decline at higher turbulence levels as capture success declines. Turbulence levels will also influence the rate of DIN and DON diffusion to the cells. These kinds of effects could give rise to much more complex impacts on *Pfiesteria* population dynamics.

According to our model, top-down control effects are very significant, i.e., direct microzooplankton grazing can dramatically reduce *Pfiesteria* zoospore populations. These results are in agreement with those of Stoecker et al. (2000, 2002) and Stoecker and Gustafson (2002) and the general idea that plankton blooms can only happen in the absence of substantial grazing control. In contrast, significant trophic cascade effects appear to be quite small due to compensatory grazing effects of *Acartia*, which removes microzooplankton but also grazes directly on *Pfiesteria*, diatoms and

cryptophytes. The model reveals significant trophic cascade effects only when it is assumed that the TOX-A functional type is grazed less by *Acartia*, which is an open question (Mallin, 1995; Roman et al., 2006). Given the tenuous nature of our understanding of the role of trophic cascades in marine ecosystem plankton dynamics, and the fact that *Acartia* represents only one of many potential grazers in a complex food web, it is difficult to draw any firm conclusions about the role of a trophic cascade in controlling *Pfiesteria* population dynamics from our model.

In general, these model experiments suggest that non-toxic blooms are more likely to occur in more turbulent inorganic-nutrient rich conditions, which are often found in more open coastal and estuarine waters that are subject to high inorganic nutrient loading, e.g., from sewage treatment plants and other point sources. In contrast, toxic blooms are more likely to occur in calm, organic-nutrient rich conditions, which are often found in shallow, protected tributaries that are subject to high organic nutrient loading, e.g., from direct runoff from animal waste and excrement-based fertilizers. It is of note that Glibert et al. (2004) found for the Chesapeake and Coastal Bays of Maryland that the average urea concentration was an excellent predictor of the percent positive detection for *Pfiesteria* spp. in the sediment of all stations monitored over a 3-year period ($R^2 \geq 0.94$), although no differentiation was made in that study of toxicity status.

The absence of strong direct grazing pressure was a prerequisite for net *Pfiesteria* population growth in all of our model experiments, but the results also support the idea that, once initiated, the formation of toxic blooms may be further promoted by inhibition of grazing pressure. These results are therefore generally consistent with observed patterns of toxic *Pfiesteria* blooms in Chesapeake Bay, the Neuse River of North Carolina and many other coastal and estuarine environments (Burkholder and Glasgow, 1997; Glibert et al., 2001, 2004).

Acknowledgements

This research was supported by R.R. Hood's component of NOAA-ECOHAB grant no. NA86OP049 to the University of Maryland Center for Environmental Science. Additional support was provided by NOAA-MERHAB grant no. NA05NOS4781222 to R.R. Hood. We also thank the Ecosystem Shortcasting and Assessment Program, a NOAA-UMCES partnership, for supporting X. Zhang during the final stage of this research. This paper represents contribution number

187 from the ECOHAB Program and 3966 from the University of Maryland Center for Environmental Science.

References

- Adolf, J.E., Stoecker, D.K., Harding Jr., L.W., 2003. Autotrophic growth and photoacclimation in *Karlodinium micrum* (dinophyceae) and *Storeatula major* (cryptophyceae). *J. Phycol.* 39, 1101–1108.
- Anderson, D.M., 1989. Toxic algal blooms and red tides: a global perspective. In: Okaichi, T., Anderson, D.M., Nemoto, T. (Eds.), *Red Tides: Biology, Environmental Science and Toxicology*. Elsevier, New York, pp. 11–16.
- Anderson, D.A., Glibert, P.M., Burkholder, J.M., 2002. Harmful algal blooms and eutrophication: Nutrient sources, composition, and consequences. *Estuaries* 25, 562–584.
- Anderson, J.T., Hood, R.R., Zhang, X., 2003. Quantification of *Pfiesteria piscicida* growth and encystment parameters using a numerical model. *Marine Ecol. Progress Ser.* (246), 105–113.
- Berg, G.M., Bakode, M., Purina, I., Bekere, S., Bechamin, C., Maestrini, S.Y., 2003. Plankton community composition in relation to availability and uptake of oxidized and reduced nitrogen. *Aquat. Microb. Ecol.* 30, 263–274.
- Bronk, D.A., Glibert, P.M., Ward, B.B., 1996. Nitrogen uptake, dissolved organic nitrogen release, and new production. *Science* 265, 1843–1846.
- Burkholder, J.M., Glasgow, H.B., 1995. Interactions of a toxic estuarine dinoflagellate with microbial predators and prey. *Arch. Protistenkd.* 145, 177–188.
- Burkholder, J.M., Glasgow, H.B., Hobbs, C.W., 1995. Fish kills linked to a toxic ambush-predator dinoflagellate: distribution and environmental conditions. *Marine Ecol. Progress Ser.* 124, 42–61.
- Burkholder, J.M., Glasgow, H.B., 1997. The ichthyotoxic dinoflagellate *Pfiesteria piscicida*: behavior, impacts and environmental controls. *Limnol. Oceanogr.* 42, 1052–1075.
- Burkholder, J.M., Glasgow, H.B., Deamer-Melia, N.J., 2001a. Overview and present status of the toxic *Pfiesteria* complex. *Phycologia* 40, 186–214.
- Burkholder, J.M., Glasgow, H.B., Deamer-Melia, N.J., Springer, J., Parrow, M.W., Zheng, C., Cancellieri, P., 2001b. Species of the toxic *Pfiesteria* complex, and the importance of functional type in data interpretations. *Environ. Health Perspect.* 109 (Suppl. 5), 667–679.
- Calbet, A., Landry, M.R., 1999. Mesozooplankton influences on the microbial food web: direct and indirect trophic interactions in the oligotrophic open ocean. *Limnol. Oceanogr.* 44, 1370–1380.
- Carpenter, S.R., Kitchell, J.F., Hodgson, J.R., 1985. Cascading trophic interactions and lake productivity. *Bioscience* 35, 1176–1180.
- Cochlan, W.P., Price, N.M., Harrison, P.J., 1991. Effects of irradiance on nitrogen uptake by phytoplankton—comparisons of frontal and stratified communities. *Marine Ecol. Progr. Ser.* 69, 103–116.
- Collos, Y., Vaquer, A., Bibent, B., Slawyk, G., Garcia, N., Souchu, P., 1997. Variability in nitrate uptake kinetics of phytoplankton communities in a Mediterranean coastal lagoon. *Estuarine Coastal Shelf Sci.* 44, 369–375.
- Feigenbaum, D., Kelly, K., 1984. Changes in the lower Chesapeake Bay food chain in presence of the sea nettle *Chrysaora quinquecirrha* (Scyphomedusa). *Marine Ecol. Progress Ser.* 19, 39–47.
- Feinstein, T.N., Traslavina, R., Sun, M.-Y., Lin, S., 2002. Effects of light on photosynthesis, grazing, and population dynamics of the

- heterotrophic dinoflagellate *Pfiesteria piscicida* (dinophyceae). J. Phycol. 38, 659–669.
- Fiksen, O., MacKenzie, B.R., 2002. Process-based models of feeding and prey selection in larval fish. Marine Ecol. Progr. Ser. 243, 151–164.
- Glibert, P.M., 1998. Interactions of top-down and bottom-up control in planktonic nitrogen cycling. Hydrobiologia 363, 1–12.
- Glibert, P.M., Alexander, J., Trice, T.M., Michael, B., Magnien, R.E., Lane, L., Oldach, D., Bowers, H., 2004. Chronic urea nitrogen loading: a correlate of *Pfiesteria* spp. in the Chesapeake and Coastal Bays of Maryland, USA. In: Steidinger, K.A., Landsberg, J.H., Tomas, C.R., Vargo, G.A. (Eds.), Harmful Algae 2002, Proceedings of the Xth International Conference on Harmful Algae, Florida Fish and Wildlife Conservation Commission and Intergovernmental Oceanographic Commission of UNESCO, pp. 74–76.
- Glibert, P.M., Anderson, D.M., Gentien, P., Graneli, E., Sellner, K.G., 2005a. The global, complex phenomena of harmful algal blooms. Oceanography 18 (2), 136–147.
- Glibert, P.M., Burkholder, J.M., 2006. The complex relationships between increasing fertilization of the Earth, coastal eutrophication and proliferation of harmful algal blooms. In: Graneli, E., Turner, J. (Eds.), Ecology of Harmful Algae. Springer.
- Glibert, P.M., Burkholder, J.M., Parrow, M.W., Lewitus, A.J., Gustafson, D., 2006. Rates of direct uptake of nitrogen and nitrogen nutritional preferences by *Pfiesteria piscicida* and *Pfiesteria shumwayae*. Harmful Algae, this issue.
- Glibert, P.M., Magnien, R., Lomas, M.W., Alexander, J., Fan, C., Haramoto, E., Trice, M., Kana, T.M., 2001. Harmful algal blooms in the Chesapeake and Coastal Bays of Maryland, USA: comparisons of 1997, 1998, and 1999 events. Estuaries 24, 875–883.
- Glibert, P.M., Seitzinger, S., Heil, C.A., Burkholder, J.M., Parrow, M.W., Codispoti, L.A., Kelly, V., 2005b. The role of eutrophication in the global proliferation of harmful algal blooms: new perspectives and new approaches. Oceanography 18 (2), 198–209.
- Glibert, P.M., Trice, T.M., Michael, B., Lane, L., 2005c. Urea in the tributaries of the Chesapeake and Coastal Bays of Maryland. Water, Air and Soil Poll. 160, 229–243.
- Gordon, A.S., Dyer, B., 2005. Relative contribution of exotoxin and micropredation to ichthyotoxicity of two strains of *Pfiesteria shumwayae* (Dinophyceae). Harmful Algae 4, 423–431.
- Hallegraeff, G.M., 1993. A review of harmful algal blooms and their apparent global increase. Phycologia 32, 79–99.
- Hood, R.R., Bates, N.R., Capone, D.G., Olson, D.B., 2001. Modeling the effect of nitrogen fixation on carbon and nitrogen fluxes at BATS. Deep-Sea Res., Part II 48, 1609–1648.
- Hood, R.R., Abbott, M.R., Huyer, A., 1991. Phytoplankton and photosynthetic light response in the coastal transition zone off northern California in June 1987. J. Geophys. Res. 96 (C8), 14769–14780.
- Lewitus, A.J., Burkholder, J.M., Glasgow, H.B., Glibert, P.M., Willis, B.M., Hayes, K.C., Burke, M., 1999a. Mixotrophy and nitrogen uptake by *Pfiesteria piscicida* (Dinophyceae). J. Phycol. 35, 1430–1437.
- Lewitus, A.J., Glasgow Jr., H.G., Burkholder, J.M., 1999b. Kleptoplastidy in the toxic dinoflagellate, *Pfiesteria piscicida* (Dinophyceae). J. Phycol. 35, 303–312.
- Lewitus, A.J., Jesien, R.V., Kana, T.M., Burkholder, J.M., Glasgow, H.B., May, E., 1995. Discovery of the phantom dinoflagellate in Chesapeake Bay. Estuaries 18, 373–378.
- Lewitus, A.J., Wetz, M.S., Willis, B.M., Burkholder, J.M., Glasgow, H.B., 2006. Grazing activity of *Pfiesteria piscicida* (Dinophyceae) and susceptibility to ciliate predation vary with toxicity status. Harmful Algae, this issue.
- Lin, S., Mulholland, M.R., Zhang, H., Feinstein, T.N., Jochem, F.J., Carpenter, E.J., 2004. Intense grazing and prey-dependent growth of *Pfiesteria piscicida* (dinophyceae). J. Phycol. 40, 1062–1073.
- Lomas, M.W., Glibert, P.M., 1999. Temperature regulation of nitrate uptake: A novel hypotheses about nitrate uptake and reduction in cool-water diatoms. Limnol. Oceanogr. 44, 556–572.
- Lomas, M.W., Rumbley, C.J., Glibert, P.M., 2000. Ammonium release by nitrogen sufficient diatoms in response to rapid increases in irradiance. J. Plank. Res. 22, 2351–2366.
- Magnien, R.E., 2001. The dynamics of scence, perception and policy during the outbreak of *Pfiesteria* in Chesapeake Bay. BioScience 51, 843–852.
- Mallin, M.A., 2000a. Impacts of industrial animal production on rivers and estuaries. Am. Sci. 88, 2–13.
- Mallin, M.A., 1995. Response of two zooplankton grazers to an ichthyotoxic estuarine dinoflagellate. J. Plank. Res. 17 (2), 351–363.
- Mallin, M.A., 2000b. Impacts of industrial-scale swine and poultry production on rivers and estuaries. Am. Sci. 88, 26–37.
- McCreary Jr., J.P., Kohler, K.E., Hood, R.R., Olson, D.B., 1996. A four-component ecosystem model of biological activity in the Arabian Sea. Progress Oceanogr. 37, 193–240.
- Purcell, J.E., Decker, M.B., 2005. Effects of climate on relative predation by scyphomedusae and ctenophores on copepods in Chesapeake Bay during 1987–2000. Limnol. Oceanogr. 50, 376–387.
- Roman, M.R., Reaugh, M.L., Zhang, X., 2006. Ingestion of the dinoflagellate, *Pfiesteria piscicida*, by the calanoid copepod, *Acartia tonsa*. Harmful Algae, this issue.
- Skelton, H., Parrow, M.W., Burkholder, J.M., 2006. Phosphatase activity in the heterotrophic dinoflagellate *Pfiesteria shumwayae* (Dinophyceae). Harmful Algae, this issue.
- Stoecker, D.K., Gustafson, D.E., 2002. Predicting grazing mortality of an estuarine dinoflagellate, *Pfiesteria piscicida*. Mar. Ecol. Progress Ser. 233, 31–38.
- Stoecker, D.K., Long, A., Suttles, S.E., Sanford, L.P., 2006. Effect of small-scale shear on grazing and growth of the dinoflagellate *Pfiesteria piscicida*. Harm. Algae, this issue.
- Stoecker, D.K., Parrow, M.W., Burkholder, J.M., Glasgow Jr., H.B., 2002. Grazing by microzooplankton on *Pfiesteria piscicida* cultures with different histories of toxicity. Aquat. Microb. Ecol. 28, 79–85.
- Stoecker, D.K., Stevens, K., Gustafson Jr., D.E., 2000. Grazing on *Pfiesteria piscicida* by microzooplankton. Aquat. Microb. Ecol. 22, 261–270.
- Smayda, T., 1990. Novel and nuisance phytoplankton blooms in the sea: evidence for a global epidemic. In: Graneli, E., Sundstrom, B., Edler, L., Anderson, D.M. (Eds.), Toxic Marine Phytoplankton. Elsevier, New York, pp. 29–40.
- Vogelbein, W.K., Lovke, V.J., Shields, J.D., Reece, K.S., Mason, P.L., Haas, L.W., Walker, C.C., 2002. *Pfiesteria shumwayae* kills fish by micropredation not exotoxin secretion. Nature 418, 967–970.
- Zhang, X., Anderson, J.T., Hood, R.R., 2003. Modeling *Pfiesteria* population dynamics: A new approach for tracking size and mass in mixotrophic species. Marine Ecol. Progress Ser. 258, 29–44.
- Zhang, X., Hood, R.E., Roman, M.R., Glibert, P.M., Stoecker, D.K., 2004. *Pfiesteria piscicida* population dynamics: A modeling study. In: Steidinger, K.A., Landsberg, J.H., Tomas, C.R., Vargo, G.A. (Eds.), Harmful Algae 2002, Proceedings of the Xth International Conference on Harmful Algae, Florida Fish and Wildlife Conservation Commission and Intergovernmental Oceanographic Commission of UNESCO, pp. 528–530.